healing of the corneal endothelium in vivo.[3] Here, we present a case of Fuchs corneal dystrophy scheduled for DSAEK surgery but successfully treated by ROCK inhibitor eye drop treatment subsequent to transcorneal freezing.

CASE REPORT

A 52-year-old Japanese man with blurred vision caused by corneal endothelial dysfunction was referred to the Kyoto Prefectural University of Medicine in May 2008. Visual acuity was 20/20 in the right eye and 20/63 in the left eye. Multiple guttae, typical of Fuchs corneal dystrophy, were observed in both eyes by slit-lamp examination and by noncontact specular microscopy (EM-3000; TOMEY Corporation, Nagoya, Japan) (Figs. 1A, B). The right cornea was clear, although the corneal endothelial density was 632 cells per square millimeter. The left cornea showed severe central edema accompanied by epithelial bullae (Figs. 2A, B). The central corneal thickness was 703 μm in the affected left eye of the patient. We were unable to perform specular microscopy in the central cornea owing to the edema, but endothelial cells were observed in the midperiphery at a density of 757 cells per square millimeter (Fig. 1B). The patient was diagnosed with late-onset Fuchs corneal dystrophy.[4] He was scheduled to have a DSAEK, but in April 2010, he volunteered for an investigative clinical study of a ROCK inhibitor eye drop treatment.

Treatment was initiated on May 18, 2010, according to a protocol approved by the Institutional Review Board of the Kyoto Prefectural University of Medicine. First, diseased corneal endothelium in the prepupillary region was removed by transcorneal freezing[3] by gently pressing a 2-mm-diameter stainless steel rod, which had been cooled in liquid nitrogen onto the corneal surface

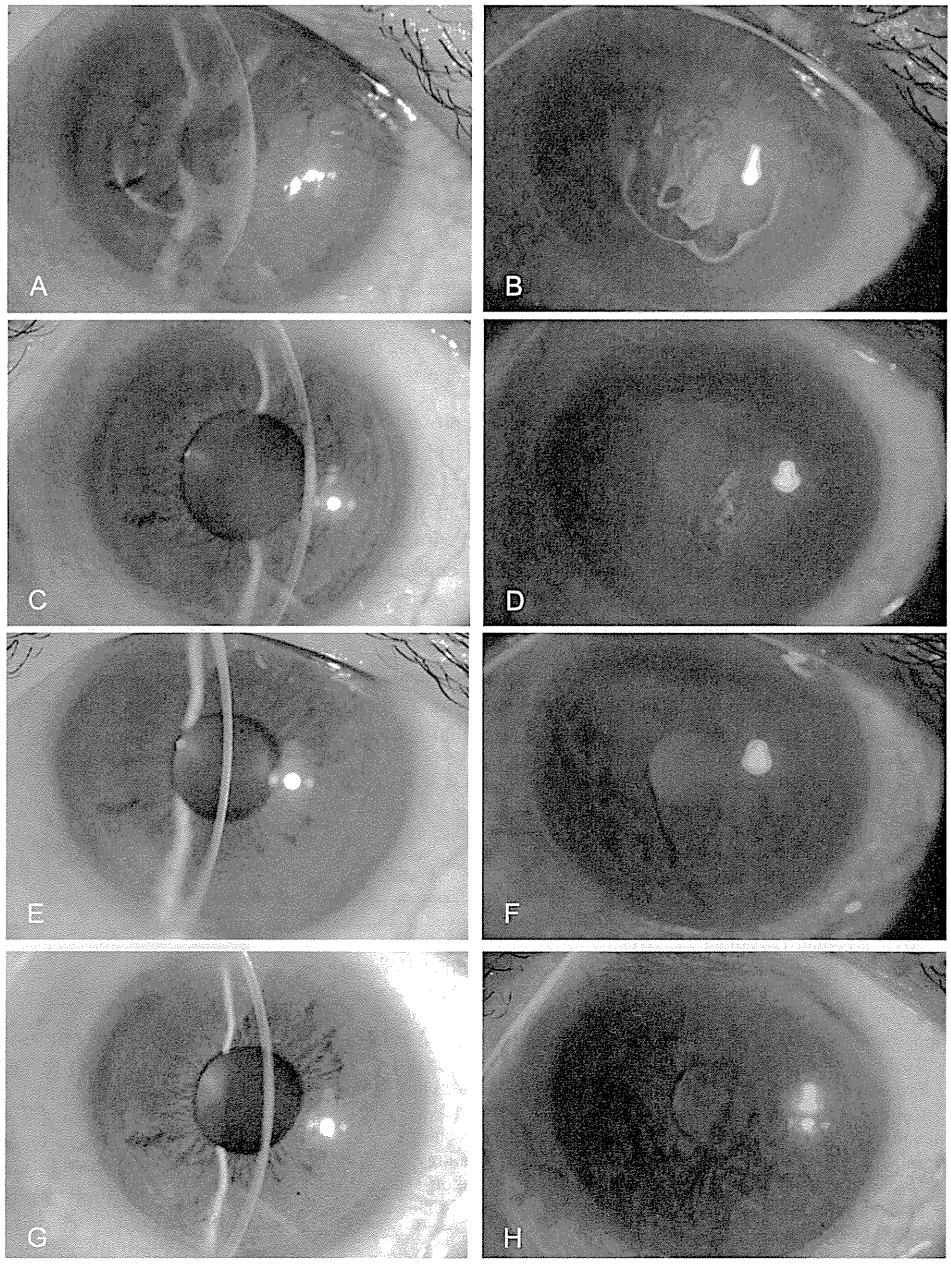

FIGURE 2. Slit-lamp photographs of our Fuchs corneal dystrophy patient before and after transcorneal freezing and ROCK inhibitor treatment. Before treatment, central corneal edema (A) accompanied by a lesion of epithelial bullae (B) was detected. C, D, Three days after the treatment, the corneal erosion created by the transcorneal freezing had already healed, and mild bullae were detected. It should be noted that less corneal edema was observed at 3 days compared with the pretreatment photograph. E, Six months after the treatment, corneal edema was significantly reduced, and cornea had recovered its clarity. F, No epithelial damage was observed by fluorescein staining. G, H, Two years after the treatment, the patient's cornea remains clear with good (20/16) vision.

for 15 seconds. In our previous study using a rabbit model, we confirmed that this transcorneal freezing procedure could make an endothelial defect of approximately the same size as the rod diameter in a reproducible fashion.[3] After the rod was removed and after the cornea had thawed, 50 μL of 10 mM ROCK inhibitor, Y-27632 (Wako, Osaka, Japan), was applied topically as eye drops, repeated 6 times daily for 7 days (May 18–24, 2010). To prevent corneal infection, 0.3% gatifloxacin hydrate eye drops were also applied 4 times daily. Epithelial erosion was detected after transcorneal freezing but had healed by posttreatment day 3 (Figs. 2C, D). No side effects, such as persistent epithelial defects or corneal stromal scars, were observed.

The patient's cornea recovered complete clarity 2 weeks after the treatment, and vision had improved to 20/20. Six months after the treatment, central corneal thickness was 568 μm, significantly lower than its pretreatment value. At this time, vision had improved to 20/16 (Figs. 2E, F). Wide-field endothelial examinations 18 months after the treatment using contact specular microscopy (Konan Medical, Inc, Nishinomiya, Japan; Fig. 3A) showed that the average corneal endothelial densities in the central and peripheral cornea were 1549.3 ± 89.7 and 705 ± 61.1 cells per square millimeter, respectively (mean ± standard error of the mean; Fig. 3B). Although Fuchs corneal dystrophy is a progressive disease, in our patient, corneal clarity and good vision (20/16) have been maintained up to the most recent observation, 2-years after the treatment (Figs. 1G, H).

DISCUSSION

ROCKs are protein serine/threonine kinases, which are the first identified and best-characterized Rho downstream effectors. The Rho/ROCK pathway is involved in regulating the cytoskeleton and has an influence on cell migration, apoptosis, and proliferation.[5–8]

We previously reported that a selective ROCK inhibitor, Y-27632, promoted the proliferation of primate corneal endothelial cells in vitro.[2] In our previous experiments, Y-27632 promoted cell proliferation up to the time when cells became preconfluent but did not promote proliferation in confluent cells whose proliferation had been stopped by contact inhibition. Based on this, and on the results of experiments in rabbits,[3] we hypothesized that the topical application of Y-27632 as an eye drop, combined with the prior partial denudation of diseased corneal endothelial cells, might be useful to promote the proliferation in situ of the corneal endothelium, which is in the early diseased phase. Thus, we came up with the protocol reported here, which shows some potential for the new approach to treat certain types of corneal endothelial dysfunction.

In the posttreatment observation of the presented case, contact specular microscopy revealed relatively small corneal endothelial cells, present at a high cell density, in the central part of cornea from where corneal endothelial cells had been removed by transcorneal freezing. The potential of topical application of ROCK inhibitor suggested by the current report clearly requires a larger comparative study to prove the effect of this new treatment, and plans are underway to conduct this. Regarding the mechanism of action of the procedure, we should also point out that spontaneous remodeling of the human corneal endothelial cells after Descemet stripping has been reported.[9,10] Based on these reports, and also bearing in mind the existence of corneal endothelial precursors with higher proliferative ability in the peripheral cornea,[11,12] we cannot rule out the possibility that reestablishment of this patient's endothelium was not a direct result of ROCK inhibitor administration, but it was the consequence of denudation of the pathologic endothelial cells. Not withstanding the preliminary nature of the current observation, this case report suggests the possibility of a medical treatment for the early phase of diseases, such as Fuchs corneal dystrophy, via the stimulation of nonaffected peripheral cells with ROCK inhibitor after the destruction of diseased cells in the central endothelium by transcorneal freezing.

To the best of our knowledge, this is the first report suggesting that the in vivo proliferation of a patient's corneal endothelium can be stimulated by interventional medical/pharmaceutical treatment after the destruction of diseased

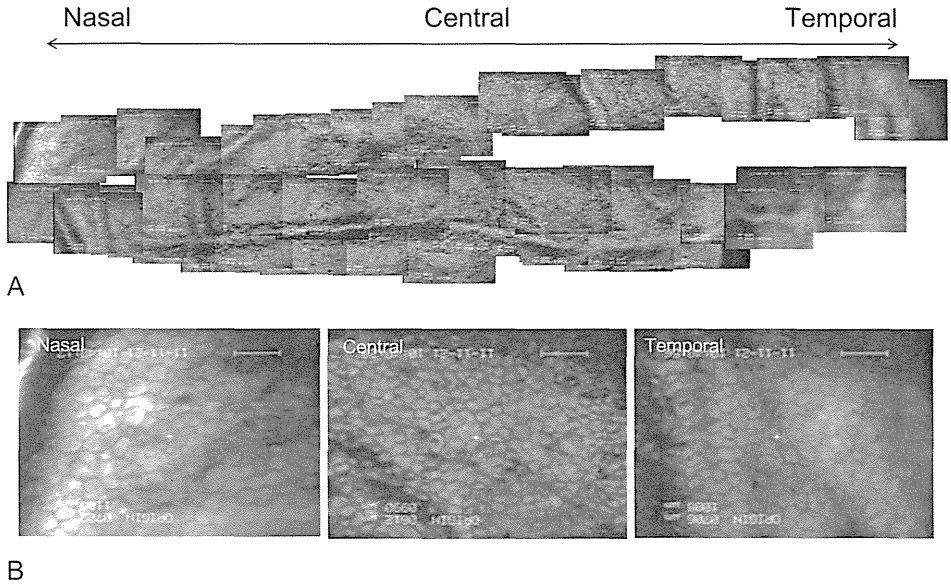

FIGURE 3. A, Wide-field observation of the corneal endothelium by contact-specular microscopy 18 months after the treatment. Guttae were detected mainly in the paracentral area. B, Representative, magnified photographs from nasal peripheral, central, and temporal peripheral area. Smaller cells, present at high density, were observed in the central cornea (scale bar =100 μm).

endothelium. We believe that our new findings will contribute to the opening up of a new approach to the treatment of corneal endothelial dysfunction.

ACKNOWLEDGMENTS

The authors thank Dr. Yoshiki Sasai (RIKEN CDB, Japan) for his invaluable advice regarding ROCK inhibitors and Prof. Andrew Quantock (Cardiff University, United Kingdom) for useful discussions.

REFERENCES

1. Terry MA, Chen ES, Shamie N, et al. Endothelial cell loss after Descemet's stripping endothelial keratoplasty in a large prospective series. *Ophthalmology.* 2008;115:488–496.
2. Okumura N, Ueno M, Koizumi N, et al. Enhancement on primate corneal endothelial cell survival in vitro by a ROCK inhibitor. *Invest Ophthalmol Vis Sci.* 2009;50:3680–3687.
3. Okumura N, Koizumi N, Ueno M, et al. Enhancement of corneal endothelium wound healing by Rho-associated kinase (ROCK) inhibitor eye drops. *Br J Ophthalmol.* 2011;95:1006–1009.
4. Eghrari AO, Gottsch JD. Fuchs' corneal dystrophy. *Expert Rev Ophthalmol.* 2010;5:147–159.
5. Coleman ML, Marshall CJ, Olson MF. RAS and RHO GTPases in G1-phase cell-cycle regulation. *Nat Rev Mol Cell Biol.* 2004;5:355–366.
6. Hall A. Rho GTPases and the actin cytoskeleton. *Science* 1998;279:509–514.
7. Olson MF, Ashworth A, Hall A. An essential role for Rho, Rac, and Cdc42 GTPases in cell cycle progression through G1. *Science.* 1995;269:1270–1272.
8. Watanabe K, Ueno M, Kamiya D, et al. A ROCK inhibitor permits survival of dissociated human embryonic stem cells. *Nat Biotechnol.* 2007;25:681–686.
9. Balachandran C, Ham L, Verschoor CA, et al. Spontaneous corneal clearance despite graft detachment in Descemet membrane endothelial keratoplasty. *Am J Ophthalmol.* 2009;148:227–234.
10. Shah RD, Randleman JB, Grossniklaus HE. Spontaneous corneal clearing after Descemet's stripping without endothelial replacement. *Ophthalmology.* 2012;119:256–260.
11. Mimura T, Joyce N. Replication competence and senescence in central and peripheral human corneal endothelium. *Invest Ophthalmol Vis Sci.* 2006;47:1387–1396.
12. Mimura T, Yamagami S, Yokoo S, et al. Comparison of rabbit corneal endothelial cell precursors in the central and peripheral cornea. *Invest Ophthalmol Vis Sci.* 2005;46:3645–3648.

PLOS ONE

Inhibition of TGF-β Signaling Enables Human Corneal Endothelial Cell Expansion *In Vitro* for Use in Regenerative Medicine

Naoki Okumura[1,2], EunDuck P. Kay[1], Makiko Nakahara[1], Junji Hamuro[2], Shigeru Kinoshita[2], Noriko Koizumi[1]*

1 Department of Biomedical Engineering, Faculty of Life and Medical Sciences, Doshisha University, Kyotanabe, Japan, **2** Department of Ophthalmology, Kyoto Prefectural University of Medicine, Kyoto, Japan

Abstract

Corneal endothelial dysfunctions occurring in patients with Fuchs' endothelial corneal dystrophy, pseudoexfoliation syndrome, corneal endotheliitis, and surgically induced corneal endothelial damage cause blindness due to the loss of endothelial function that maintains corneal transparency. Transplantation of cultivated corneal endothelial cells (CECs) has been researched to repair endothelial dysfunction in animal models, though the *in vitro* expansion of human CECs (HCECs) is a pivotal practical issue. In this study we established an optimum condition for the cultivation of HCECs. When exposed to culture conditions, both primate and human CECs showed two distinct phenotypes: contact-inhibited polygonal monolayer and fibroblastic phenotypes. The use of SB431542, a selective inhibitor of the transforming growth factor-beta (TGF-β) receptor, counteracted the fibroblastic phenotypes to the normal contact-inhibited monolayer, and these polygonal cells maintained endothelial physiological functions. Expression of ZO-1 and Na^+/K^+-ATPase maintained their subcellular localization at the plasma membrane. Furthermore, expression of type I collagen and fibronectin was greatly reduced. This present study may prove to be the substantial protocol to provide the efficient *in vitro* expansion of HCECs with an inhibitor to the TGF-β receptor, and may ultimately provide clinicians with a new therapeutic modality in regenerative medicine for the treatment of corneal endothelial dysfunctions.

Citation: Okumura N, Kay EP, Nakahara M, Hamuro J, Kinoshita S, et al. (2013) Inhibition of TGF-β Signaling Enables Human Corneal Endothelial Cell Expansion *In Vitro* for Use in Regenerative Medicine. PLoS ONE 8(2): e58000. doi:10.1371/journal.pone.0058000

Editor: Che John Connon, University of Reading, United Kingdom

Received November 5, 2012; **Accepted** January 29, 2013; **Published** February 25, 2013

Funding: The work was supported in part by the Highway Program for realization of regenerative medicine (Kinoshita and Okumura); http://www.mext.go.jp/english/; and the Funding Program for Next Generation World-Leading Researchers from the Cabinet Office in Japan (Koizumi: LS117); http://www.jsps.go.jp/english/e-jisedai/index.html. The funders had no role in study design, data collection and analysis, decision to publish, or preparation of the manuscript.

Competing Interests: The authors have declared that no competing interests exist.

* E-mail: nkoizumi@mail.doshisha.ac.jp

Introduction

Corneal endothelial dysfunction is a major cause of severe visual impairment leading to blindness due to the loss of endothelial function that maintains corneal transparency. Restoration to clear vision requires either full-thickness corneal transplantation or endothelial keratoplasty. Recently, highly effective surgical techniques to replace corneal endothelium [e.g., Descemet's stripping automated endothelial keratoplasty (DSAEK) and Descemet's membrane endothelial keratoplasty (DMEK)] have been developed [1–3] that are aimed at replacing penetrating keratoplasty for overcoming pathological dysfunctions of corneal endothelial tissue. At present, our group and several other research groups have focused on the establishment of new treatment methods suitable for a practical clinical intervention to repair corneal endothelial dysfunctions [4–9]. Since corneal endothelium is composed of a monolayer and is a structurally flexible cell sheet, corneal endothelial cells (CECs) have been cultured on substrates including collagen sheets, amniotic membrane, or human corneal stroma. Then the cultured CECs are transplanted as a cell sheet. However, these techniques require the use of an artificial or biological substrate that may introduce several problems such as substrate transparency, detachment of the cell sheet from the cornea, and technical difficulty of transplantation into the anterior chamber. In our effort to overcome those substrate-related problems, we previously demonstrated that the transplantation of cultivated CECs in combination with a Rho kinase (ROCK) inhibitor enhanced the adhesion of injected cells onto the recipient corneal tissue without the use of a substrate and successfully achieved the recovery of corneal transparency in two corneal-endothelial-dysfunction animal models (rabbit and primate) [10,11].

However, in the context of the clinical setting, another pivotal practical issue is the *in vitro* expansion of human CECs (HCECs). HCECs are vulnerable to morphological fibroblastic change under normal culture conditions. Although HCECs can be cultivated into a normal phenotype maintaining the contact-inhibited polygonal monolayer, they eventually undergo massive endothelial-mesenchymal transformation after long-term culture or subculture. Thus, cultivation of HCECs with normal physiological function is difficult, yet not impossible [12,13].

Epithelial mesenchymal transformation (EMT) has been well characterized in epithelial-to-mesenchymal transition, and transforming growth factor-beta (TGF-β) can initiate and maintain EMT in a variety of biological and pathological systems [14,15].

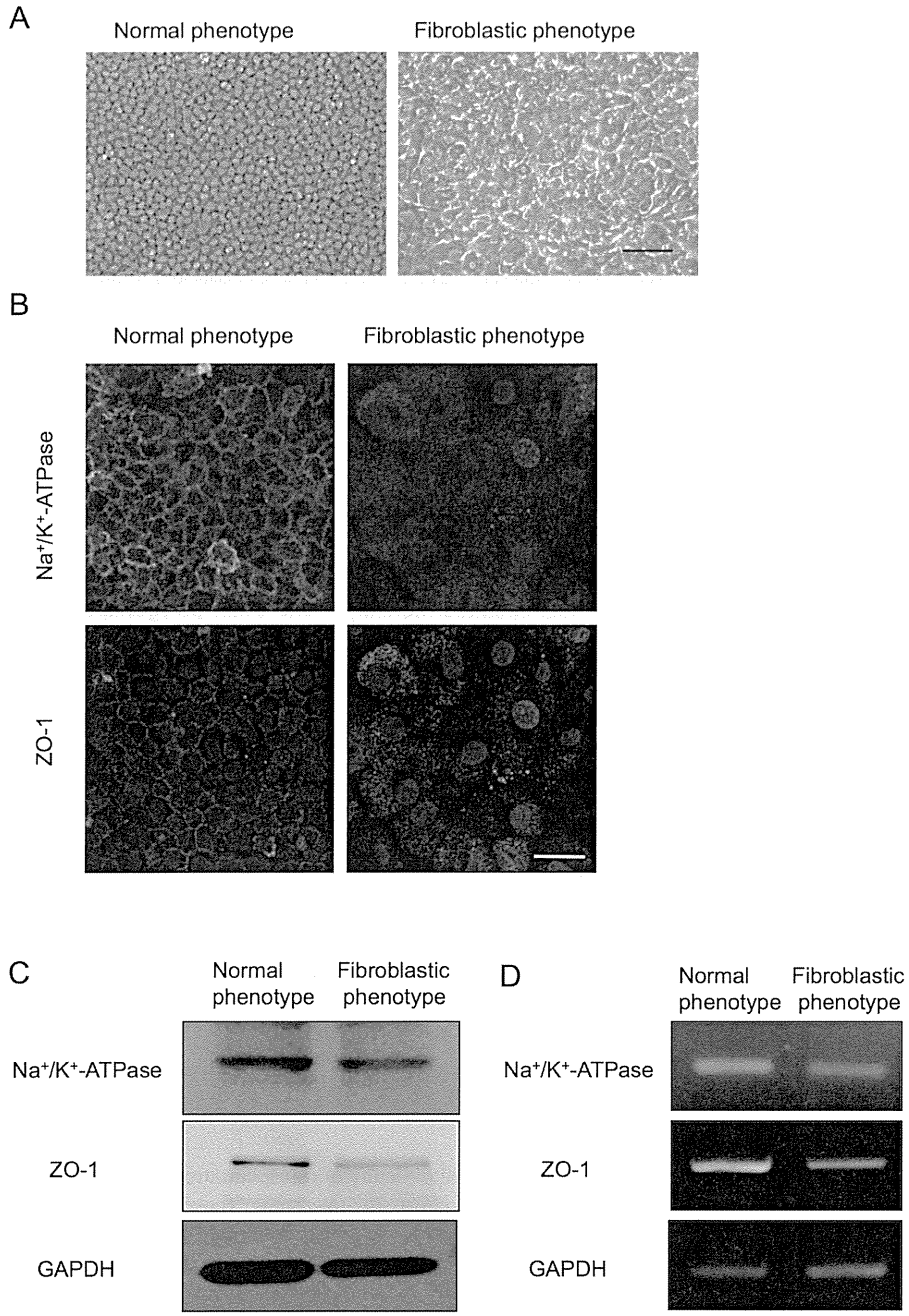

Figure 1. Primate corneal endothelial cells exhibit fibroblastic phenotype and lose functions during cell culture. (A) Cultivated primate CECs demonstrated two distinctive phenotypes; the cells maintained the characteristic polygonal cell morphology and contact-inhibited phenotype (normal phenotype) and the cells showed a fibroblastic cell shape with multi-layering (fibroblastic phenotype). Both phenotypes of the cultured CECs were primary cultured cells. Scale bar: 50 μm. The experiment was performed in triplicate. (B) Na^+/K^+-ATPase and ZO-1 at the plasma membrane was preserved in the normal phenotype, while fibroblastic phenotype completely lost the characteristic staining profile of Na^+/K^+-ATPase and ZO-1 at the plasma membrane. Scale bar: 100 μm. (C+D) Expression of the Na^+/K^+-ATPase and ZO-1 was higher in normal phenotypes than in the fibroblastic phenotypes at both the protein and mRNA levels. Samples were prepared in duplicate. Immunoblotting and semiquantitative PCR were performed in duplicate.
doi:10.1371/journal.pone.0058000.g001

The cellular activity of TGF-β is of particular interest in epithelial cells, as it inhibits the G1/S transition of the cell cycle in these cells. However, the same growth factor is the key signaling molecule for EMT, and the role of TGF-β as a key molecule in the development and progression of EMT is well studied [14–17]. Smad2/3 are signaling molecules downstream of cell-surface receptors for TGF-β in epithelial-to-mesenchymal transition [16,17]. Similar to epithelial cells, TGF-β inhibits the G1/S transition of the cell cycle in CECs [18,19], however, it is not known how TGF-β develops endothelial to mesenchymal transformation and maintains it in CECs. Endothelial-mesenchymal transformation is observed among corneal endothelial dysfunctions such as Fuchs' endothelial corneal dystrophy, pseudoexfoliation syndrome, corneal endotheliitis, surgically-induced corneal

endothelial damage, and corneal trauma and it induces the fibroblastic transformation of CECs [20–23], suggesting that CECs have the biological potential to acquire endothelial to mesenchymal transformation. The apparent presence of fibroblastic phenotypes in primate CECs and HCECs in culture led us to search for the cause of such phenotypic changes of the cultivated cells and for a means in which to prevent such undesirable cellular changes toward endothelial-mesenchymal transformation.

In the present study, we established primate CEC and HCEC cultures which respectively showed two distinctive phenotypes: 1) normal and 2) fibroblastic. We further characterized the two phenotypes and showed evidence that the use of an inhibitor to TGF-β receptor or BMP-7 abolished the fibroblastic phenotypes of cultivated CECs. Thus, intervention by inhibiting the endothelial to mesenchymal transformation process that occurs during the cultivation of CECs will certainly enable the *in vitro* expansion of cultivated HCECs with a normal phenotype which would be ideal for therapeutic clinical application.

Materials and Methods

Ethics Statement

The monkey tissue used in this study was handled in accordance with the ARVO Statement for the Use of Animals in Ophthalmic and Vision Research. The isolation of the tissue was approved by an institutional animal care and use committee of the Nissei Bilis Co., Ltd. (Otsu, Japan) and the Eve Bioscience, Co., Ltd. (Hashimoto, Japan). The human tissue used in this study was handled in accordance with the tenets set forth in the Declaration of Helsinki. A written consent was acquired from the next of kin of all deceased donors regarding eye donation for research. All tissue is recovered under the tenants of the Uniform Anatomical Gift Act (UAGA) of the particular state where the donor was consented and recovered.

Monkey cornea tissues and Research-grade human cornea tissues

Eight corneas from 4 cynomolgus monkeys (3 to 5 years-of-age; estimated equivalent human age: 5 to 20 years) housed at Nissei Bilis and the Keari Co., Ltd., Osaka, Japan, respectively, were used for the MCECs culture. The cynomolgus monkeys were housed in individual stainless steel cages at Nissei Bilis and Eve Bioscience. Each cage was provided with reverse-osmosis water delivered by an automatic water supply system and supplied with experimental animal diet (PS-A; Oriental Yeast Co., Ltd., Tokyo, Japan). Room temperature was controlled by heating units inside the rooms and was maintained at 18.0–26.0°C. The humidity was maintained at 29.5 to 80.4%. Animals were maintained on a 12:12-h light:dark cycle (lights on, 7 a.m. to 19 p.m.). For other research purposes, the animals were given an overdose of intravenous pentobarbital sodium for euthanatization. The corneas of cynomolgus monkeys were harvested after confirmation of cardiopulmonary arrest by veterinarians, and then provided for our research. Twenty human donor corneas were obtained from the SightLife™ (Seattle, WA) eye bank, and all corneas were stored at 4°C in storage medium (Optisol; Chiron Vision Corporation, Irvine, CA) for less than 14 days prior to the primary culture.

Cell culture of monkey CECs (MCECs)

The MCECs were cultivated in modified protocol as described previously [7,24]. Briefly, the Descemet's membrane including CECs was stripped and digested at 37°C for 2 h with 1 mg/mL collagenase A (Roche Applied Science, Penzberg, Germany). After a digestion at 37°C, the MCECs obtained from individual corneas were resuspended in culture medium and plated in 1 well of a 6-well plate coated with FNC Coating Mix® (Athena Environmental

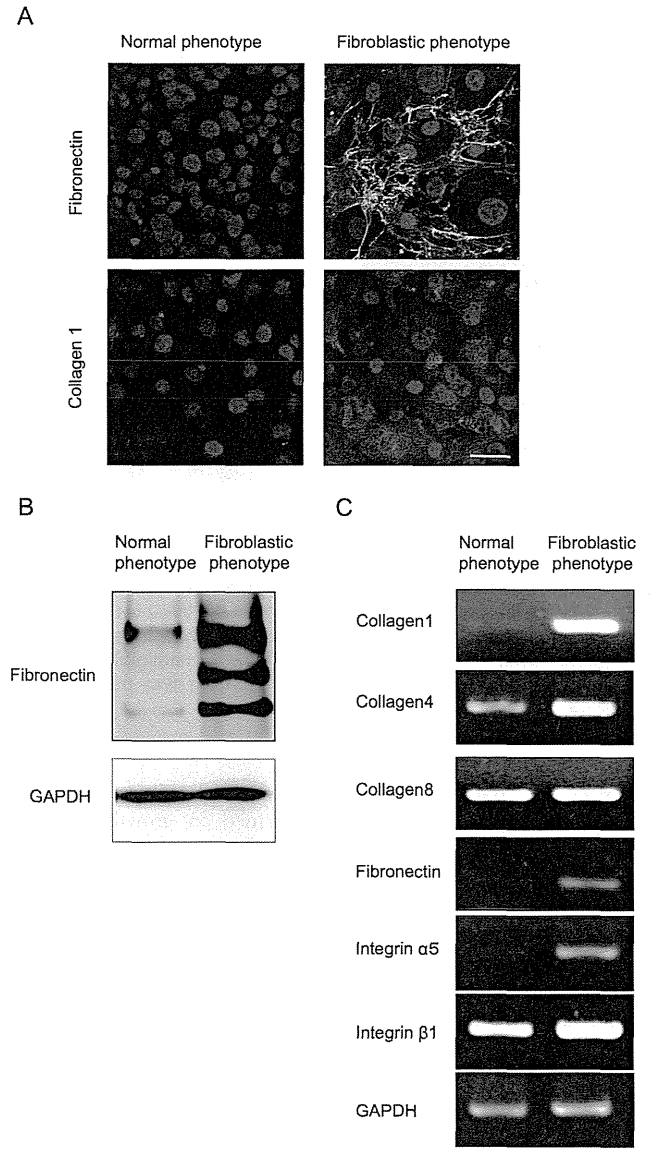

Figure 2. Fibroblastic primate CECs produced an abnormal extra cellular matrix. (A) The fibroblastic phenotype demonstrated excessive ECMs such as fibronectin and collagen type 1, while the normal phenotype completely lost the staining potential. Scale bar: 100 μm. (B) The protein expression level of fibronectin was more strongly upregulated in the fibroblastic phenotype than in the normal phenotype. (C) Semiquantitative PCR analysis showed that the type I collagen transcript [α1(I) mRNA] was abundantly expressed in the fibroblastic phenotypes, while the expression of α1(I) mRNA was reduced in the normal phenotypes. The basement membrane collagen phenotype α1(IV) mRNA was expressed both in normal and fibroblastic phenotypes, yet to a lesser degree in the normal phenotype. Collagen phenotype α1(VIII) mRNA was expressed in both phenotypes at similar levels. Fibronectin and integrin α5 mRNA was observed in the fibroblastic phenotypes, as opposed to the normal phenotypes in which the two transcripts were not expressed. β1 integrin mRNA was expressed in both phenotypes at similar levels. Samples were prepared in duplicate. Immunoblotting and semiquantitative PCR were performed in duplicate.
doi:10.1371/journal.pone.0058000.g002

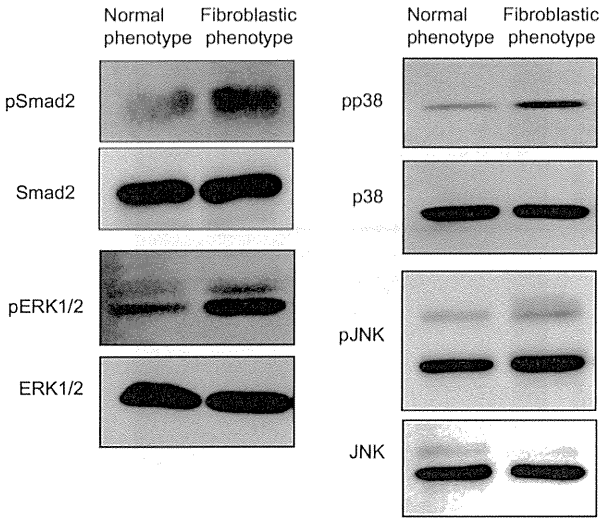

Figure 3. Different activation pattern of fibroblastic change associated pathways in the fibroblastic phenotype of primate CECs. Phosphorylation of Smad2, p38MAPK, and ERK1/2 was promoted in the fibroblastic phenotype compared to that in the normal phenotype, while phosphorylation of JNK was negligible. Samples were prepared in duplicate, and immunoblotting was performed in duplicate.
doi:10.1371/journal.pone.0058000.g003

Sciences, Inc., Baltimore, MD). All primary cell cultures and serial passages of the MCECs were performed in growth medium composed of Dulbecco's modified Eagle's medium (Invitrogen Corporation, Carlsbad, CA) supplemented with 10% fetal bovine serum (FBS), 50 U/mL penicillin, 50 μg/mL streptomycin, and 2 ng/mL FGF-2 (Invitrogen). The MCECs were then cultured in a humidified atmosphere at 37°C in 5% CO_2, and the culture medium was changed every 2 days. When the MCECs reached confluency in 10 to 14 days, they were rinsed in Ca^{2+} and Mg^{2+}-free Dulbecco's phosphate-buffered saline (PBS), trypsinized with 0.05% Trypsin-EDTA (Invitrogen) for 5 min at 37°C, and passaged at ratios of 1:2–4. Cultivated MCECs at passages 2 through 5 were used for all experiments. SB431542 (Merck Millipore, Billerica, MA), a selective inhibitor of transforming growth factor-β (TGF-beta), was tested for the anti-fibroblastic effect.

Cell culture of HCECs

The HCECs were cultivated in a modified version of the protocol used for the MCECs. Briefly, the Descemet's membrane including CECs was stripped and digested at 37°C for 2 h with 1 mg/mL collagenase A (Roche Applied Science). After a digestion at 37°C, the HCECs obtained from individual corneas were resuspended in culture medium and plated in 1 well of a 12-well plate coated with FNC Coating Mix®. The culture medium was prepared according to published protocols [25], but with some modifications. Briefly, basal culture medium containing Opti-MEM-I (Invitrogen), 8% FBS, 5 ng/mL epidermal growth factor (EGF) (Sigma-Aldrich Co., St. Louis, MO), 20 μg/mL ascorbic acid (Sigma-Aldrich), 200 mg/L calcium chloride (Sigma-Aldrich), 0.08% chondroitin sulfate (Wako Pure Chemical Industries, Ltd., Osaka, Japan), and 50 μg/mL of gentamicin was prepared, and the conditioned medium was then recovered after cultivation of inactivated 3T3 fibroblasts. Inactivation of the 3T3 fibroblasts was performed as described previously [26,27]. Briefly, confluent 3T3 fibroblasts were incubated with 4 μg/mL mitomycin C (MMC) (Kyowa Hakkko Kirin Co., Ltd., Tokyo, Japan) for 2 h at 37°C under 5% CO_2, and then trypsinized and plated onto plastic dishes at the density of 2×10^4 cells/cm^2. The HCECs were cultured in a humidified atmosphere at 37°C in 5% CO_2, and the culture medium was changed every 2 days. When the HCECs reached confluency in 14 to 28 days, they were rinsed in Ca^{2+} and Mg^{2+}-free PBS, trypsinized with 0.05% Trypsin-EDTA for 5 min at 37°C, and passaged at ratios of 1:2. Cultivated HCECs at passages 2 through 5 were used for all experiments. To test the anti-fibroblastic effect, the cultured HCECs were passaged at the ratio of 1:2 with medium supplemented with or without SB431542 (0.1, 1, and 10 μM) (Merck Millipore), a neutralizing antibody to TGF-β (500 ng/ml) (R&D Systems, Inc., Minneapolis, MN), Smad3 inhibitor (3 mM) (Merck Millipore), and bone morphogenetic protein (BMP) BMP-7 (10, 100, and 1000 ng/ml) (R&D Systems), and were then evaluated after 1 week.

Histological examination

For histological examination, cultured MCECs or HCECs on Lab-Tek^{TM} Chamber Slides^{TM} (NUNC A/S, Roskilde, Denmark) were fixed in 4% formaldehyde for 10 min at room temperature (RT) and incubated for 30 min with 1% bovine serum albumin (BSA). To investigate the phenotype of the CECs, immunohistochemical analyses of ZO-1 (Zymed Laboratories, Inc., South San Francisco, CA), a tight junction associated protein, Na^+/K^+-ATPase (Upstate Biotechnology, Inc., Lake Placid, NY), the protein associated with pump function, fibronectin (BD, Franklin Lakes, NJ), and actin were performed. ZO-1 and Na^+/K^+-ATPase were used as function related markers of the CECs, fibronectin and collagen type 1 were used to evaluate the fibroblastic change, and actin staining was used to evaluate the cellular morphology. The ZO-1, Na^+/K^+-ATPase, collagen type 1, and fibronectin staining were performed with a 1:200 dilution of ZO-1 polyclonal antibody, Na^+/K^+-ATPase monoclonal antibody, and fibronectin monoclonal antibody, respectively. For the secondary antibody, a 1:2000 dilution of Alexa Fluor® 488-conjugated or Alexa Fluor® 594-conjugated goat anti-mouse IgG (Invitrogen) was used. Actin staining was performed with a 1:400 dilution of Alexa Fluor® 488-conjugated phalloidin (Invitrogen). Cell nuclei were then stained with DAPI (Vector Laboratories, Inc., Burlingame, CA) or propidium iodide (PI) (Sigma-Aldrich). The slides were then inspected by fluorescence microscopy (TCS SP2 AOBS; Leica Microsystems, Wetzlar, Germany). The percentages of Na^+/K^+-ATPase- and ZO-1-positive cells that expressed Na^+/K^+-ATPase and ZO-1 at the plasma membrane in the *in vivo* condition were counted by a blinded examiner.

Immunoblotting

For immunoblotting, the cells were washed with PBS and then lysed with radio immunoprecipitation assay (RIPA) buffer (Bio-Rad Laboratories, Hercules, CA) containing Phosphatase Inhibitor Cocktail 2 (Sigma-Aldrich) and Protease Inhibitor Cocktail (Nacalai Tesque, Kyoto, Japan). The lysates were then centrifuged at 15,000 rpm for 10 min at 4°C. The resultant supernatant was collected and the protein concentration of the sample was assessed with the BCA^{TM} Protein Assay Kit (Takara Bio Inc., Otsu, Japan). The proteins were then separated by sodium dodecyl sulfate polyacrylamide gel electrophoresis (SDS-PAGE) and transferred to polyvinylidene fluoride (PVDF) membranes. The membranes were then blocked with 3% non-fat dry milk (Cell Signaling Technology, Inc., Danvers, MA) in TBS-T buffer. The incubations were then performed with the following primary antibodies: Na^+/K^+-ATPase (Merck Millipore), ZO-1, GAPDH (Abcam, Cambridge, UK), fibronectin, and Smad2 (Cell Signaling Technology),

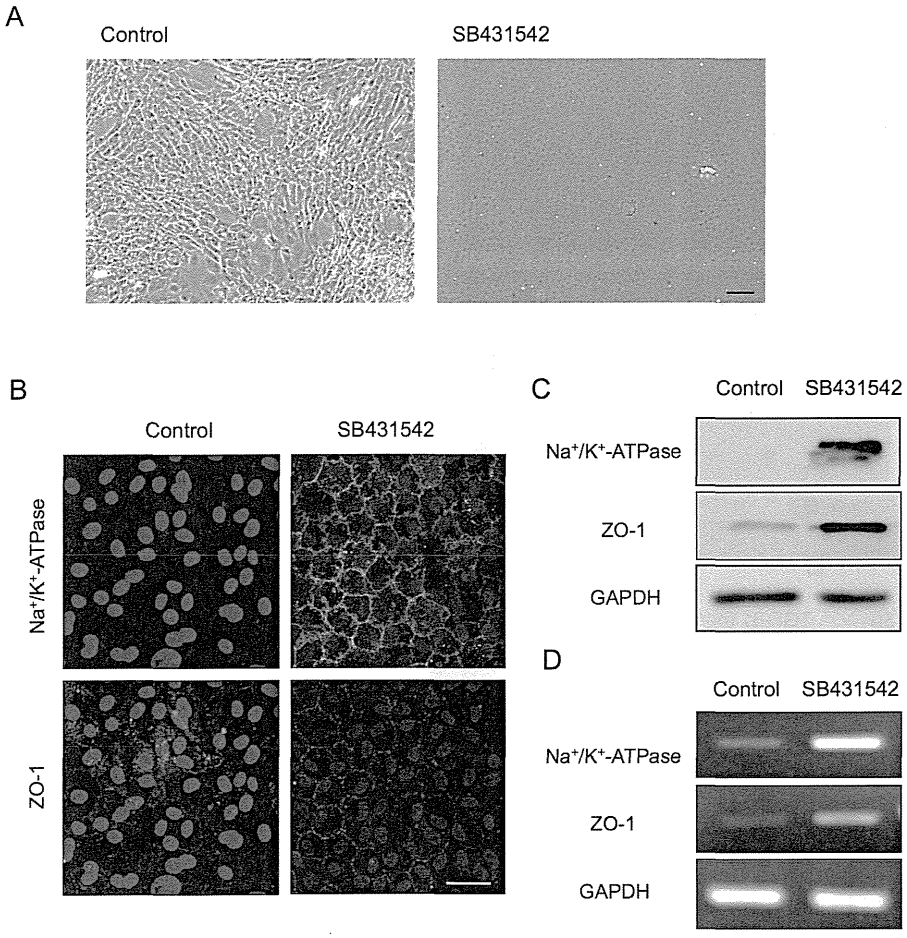

Figure 4. Inhibition of the TGF-β pathway suppressed fibroblastic change and maintained functions. (A) Primate CECs cultured with SB431542 exhibited the authentic polygonal cell shape and contact-inhibited monolayer, while the control CECs exhibited the fibroblastic morphology. Scale bar: 50 μm. (B) SB431542-treated CECs showed the characteristic plasma membrane staining of Na^+/K^+-ATPase and ZO-1, while the control CECs lost their staining. Scale bar: 100 μm. (C+D) Expression of Na^+/K^+-ATPase and ZO-1 was greatly upregulated in the SB431542-treated fibroblastic phenotypes at both the protein and mRNA levels. Samples were prepared in duplicate. Immunoblotting and semiquantitative PCR were performed in duplicate.
doi:10.1371/journal.pone.0058000.g004

phosphorylated Smad2 (Cell Signaling Technology), ERK1/2 (BD), phosphorylated ERK1/2 (BD), p38MAPK (BD), phosphorylated p38MAPK (BD) JNK (BD) or phosphorylated JNK (BD) (1:1000 dilution), and HRP-conjugated anti-rabbit or anti-rabbit IgG secondary antibody (Cell Signaling Technology) (1:5000 dilution). Membranes were exposed by ECL Advance Western Blotting Detection Kit (GE Healthcare, Piscataway, NJ), and then examined by use of the LAS4000S (Fujifilm, Tokyo, Japan) imaging system.

Semiquantitative reverse transcriptase polymerase chain reaction (RT-PCR) and quantitative PCR

Total RNA was extracted from CECs and cDNA was synthesized by use of ReverTra Ace® (Toyobo, Osaka, Japan), a highly efficient RT. The same amount of cDNA was amplified by PCR (GeneAmp 9700; Applied Biosystems) and the following primer pairs: GAPDH mRNA, forward (5′-GAGTCAACGGATTTGGTCGT-3′), and reverse (5′-TTGATTTTGGAGGGATCTCG-3′); Na^+/K^+-ATPase mRNA, forward (5′-CTTCCTCCGCATTTATGCTCATTTTCTCACCC-3′), and reverse (5′-GGATGATCATAAACTTAGCCTTGATGAACTC-3′); ZO-1 mRNA, forward (5′-GGACGAGGCATCATCCCTAA-3′), and reverse (5′-CCAGCTTCTCGAAGAACCAC-3′); collagen1 mRNA, forward (5′-TCGGCGAGAGCATGACCGATGGAT-3′), and reverse (5′-GACGCTGTAGGT GAAGCGGCTGTT-3′); collagen4 mRNA, forward (5′-AGCAAGGTGTTACAGGATTGGT -3′), and reverse (5′- AGAAGGACACTGTGGGTCATCT -3′); collagen8 mRNA, forward (5′-ATGTGATGGCTGTGCTGCTGCTGCCT -3′), and reverse (5′-CTCTTGGGCCAGGCTCTCCA-3′); fibronectin mRNA, forward (5′-AGATGAGTGGGAACGAATGTCT -3′), and reverse (5′-GAGGGTCACACTTGAATTCTCC -3′); integrin α5 mRNA, forward (5′-TCCTCAGCAAGAATCTCAACAA -3′), and reverse (5′-GTTGAGTCCCGTAACTCTGGTC -3′); integrin β1 mRNA, forward (5′-GCTGAAGACTATCCCATTGACC -3′), and reverse (5′-ATTTCCAGATATGCGCTGTTTT -3′). PCR products were analyzed by agarose gel electrophoresis. Quantitative PCR was performed using the following TaqMan® (Invitrogen) primers: collegen1, Hs00164004_m1; fibronectin, Hs01549976_m1; GAPDH, Hs00266705_g1. The PCR was performed using the StepOne™ (Applied Biosystems) real-time PCR system. GAPDH was used as an internal standard.

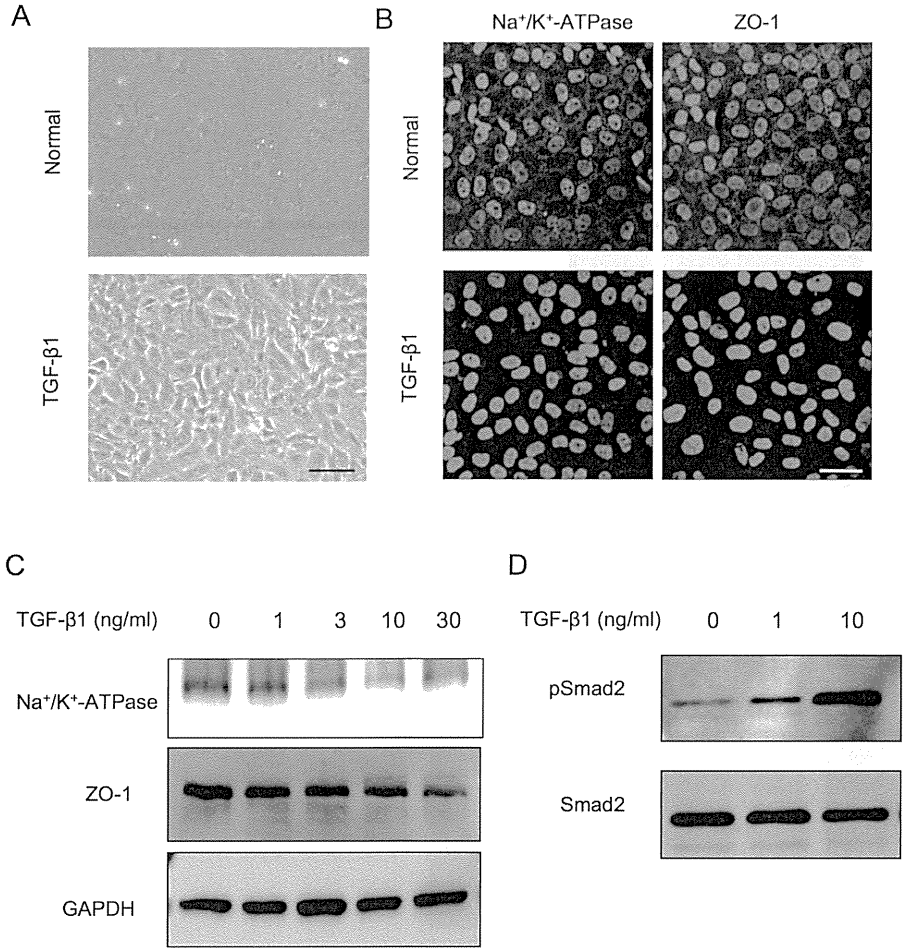

Figure 5. TGFβ induced fibroblastic change and function loss through the activation of the Smad signaling pathways. (A) Normal phenotype primate CECs were transformed to fibroblastic cells when exposed to the exogenous TGF-β1 (10 ng/ml). Scale bar: 50 μm. (B) The staining pattern of Na^+/K^+-ATPase and ZO-1 at the plasma membrane of the normal phenotypes was greatly reduced upon exposure to TGF-β1 (10 ng/ml). Scale bar: 100 μm. (C) TGF-β1 reduced the expression of Na^+/K^+-ATPase and ZO-1 at protein levels dose-dependently. (D) Phosphorylation of Smad2 was increased in a concentration-dependent manner. Samples were prepared in duplicate, and immunoblotting was performed in duplicate.
doi:10.1371/journal.pone.0058000.g005

Enzyme-linked immunosorbent assay (ELISA)

Collagen type I of culture medium supernatant of HCECs were measured using ELISA kits for Collagen Type I Alpha 2 (COL1a2) (Uscn Life Science Inc., Wuhan, China) according to the manufacturer's instructions. Culture medium supernatant from HCECs cultured with or without SB431542 were used for each group (n = 5).

Statistical analysis

The statistical significance (*P*-value) in mean values of the two-sample comparison was determined by use of the Student's t-test. The statistical significance in the comparison of multiple sample sets was analyzed by use of the Dunnett's multiple-comparisons test. Values shown on the graphs represent the mean ± SE.

Results

Two distinct phenotypes of primate CECs during cell culture

Of great interest, the primate CECs in culture demonstrated two distinctive phenotypes when determined by cell morphology and the characteristic contact-inhibited phenotype. Although to culture primate CECs in a normal phenotype while maintaining the monolayer contact-inhibited morphology is possible, they often showed morphological fibroblastic change after primary culture following isolation from the cornea, or long-term culture or subculture, if they were once primary cultured in normal morphology (Fig. 1A). The two phenotypes were then tested for the endothelial characteristics; the staining pattern of Na^+/K^+-ATPase and ZO-1 at the plasma membrane was well preserved in the normal phenotypes, yet the fibroblastic phenotypes completely lost the characteristic staining profile of Na^+/K^+-ATPase and ZO-1 at the plasma membrane (Fig. 1B). Expression of the two functional proteins was found to be much greater in the normal phenotypes than in the fibroblastic phenotypes at both the protein (Fig. 1C) and mRNA levels (Fig. 1D). Comparison of the expression of authentic fibrillar extracellular matrix (ECM) proteins showed that fibroblastic phenotypes demonstrated a fibrillar ECM staining pattern of fibronectin, while the normal phenotypes completely lost the staining potential of fibronectin (Fig. 2A). The protein expression level of fibronectin was more strongly upregulated in the fibroblastic phenotypes than in the normal phenotypes (Fig. 2B). Type I collagen produced by fibroblastic phenotypes demonstrated dual locations, at the ECM

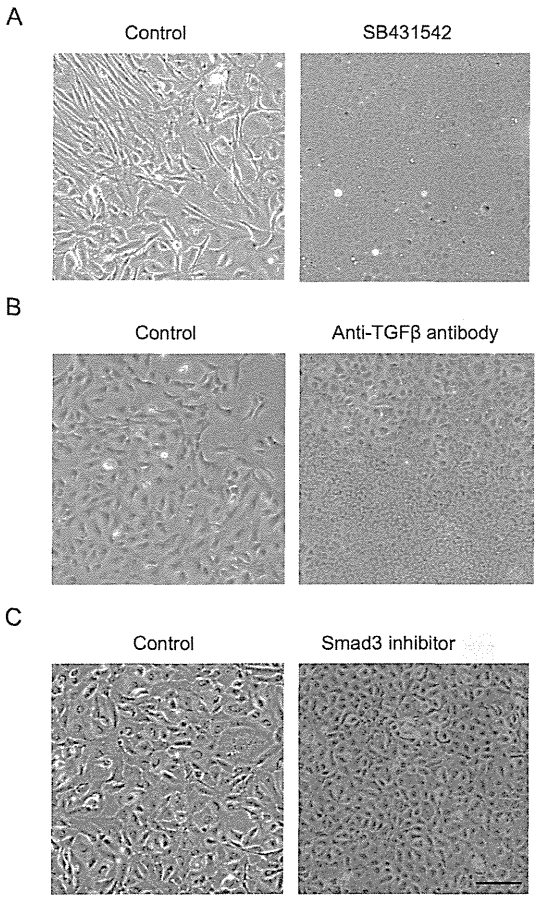

Figure 6. Inhibition of the TGFβ pathway suppressed the fibroblastic change of HCECs. (A) HCECs cultured with SB431542 (1 μM) exhibited the hexagonal cell shape and contact-inhibited monolayer, while the control CECs exhibited the fibroblastic morphology. (B+C) Both neutralizing antibody to TGF-β (500 ng/ml) and Smad3 inhibitor (3 mM) blocked cells from acquiring fibroblastic phenotypes. Scale bar: 50 μm. The experiment was performed in duplicate.
doi:10.1371/journal.pone.0058000.g006

and at the cytoplasm. Of interest, the cytoplasmic location of type I collagen appeared to be at the Golgi complex, the intracellular localization of which is essential for secretion, and these findings are similar to the published data [28]. On the other hand, type I collagen staining in the normal phenotypes was not clearly observed (Fig. 2A). RT-PCR analysis was used to determine the expression of major ECM proteins. The type I collagen transcript [α1(I) mRNA] was found to be abundantly expressed in the fibroblastic phenotypes, while the expression of α1(I) mRNA was negligible in the normal phenotypes (Fig. 2C). Unlike the type I collagen transcript, the basement membrane collagen phenotype α1(IV) mRNA was expressed in both the normal and fibroblastic phenotypes, yet to a lesser degree in the normal phenotype. Collagen phenotype α1(VIII) mRNA was expressed in both phenotypes at similar levels. Expression of fibronectin and integrin α5 was observed in the fibroblastic phenotypes, as opposed to the normal phenotypes in which the two transcripts were not expressed (Fig. 2C). On the other hand, β1 integrin mRNA was expressed in both phenotypes at similar levels (Fig. 2C).

Next, signaling pathways were determined to elucidate what might cause fibroblastic phenotypes of CECs. Since Smad2, p38, ERK1/2, and JNK are reportedly all involved in the EMT pathway [18–20,29,30], we therefore tested whether Smad2 and the MAPKs were involved in an endothelial-mesenchymal transformation similar to the EMT observed in epithelial cells (Fig. 3). Phosphorylation of Smad2 was found to be greatly promoted in the fibroblastic phenotypes when compared to that in the normal phenotypes. Phosphorylation of p38 and ERK1/2 was greatly enhanced in the fibroblastic phenotypes, while activation of JNK was negligible. These findings suggested that TGF-β signaling may exert the key role for the fibroblastic transformation of CECs.

TGF-β-mediated endothelial-mesenchymal transformation and use of TGF-β receptor inhibitor to block it in primate CECs

The findings shown in Fig. 3 led us to directly test whether SB431542, the TGF-β receptor inhibitor, was able to block the EMT process observed in the fibroblastic phenotypes. Phase contrast imaging demonstrated that primate CECs cultured in the presence of SB431542 exhibited the authentic polygonal cell shape and contact-inhibited monolayer, while the control CECs exhibited the fibroblastic morphology (Fig. 4A). Moreover, the SB431542-treated CECs showed the characteristic plasma membrane staining of Na^+/K^+-ATPase and ZO-1, while the control CECs lost their staining, suggesting that endothelial functions were maintained in the SB431542-treated cells (Fig. 4B). Furthermore, the expression of Na^+/K^+-ATPase and ZO-1 was strongly upregulated in the SB431542-treated fibroblastic phenotypes at both the protein (Fig. 4C) and mRNA levels (Fig. 4D). These data further confirmed that TGF-β might be the direct mediator of the endothelial to mesenchymal transformation observed in primate CEC cultures. Therefore, we tested whether the normal phenotypes were transformed to fibroblastic cells when exposed to the exogenous TGF-β, as in the findings shown in Fig. 5A. Of interest, the staining pattern of Na^+/K^+-ATPase and ZO-1 at the plasma membrane of the normal phenotypes was greatly reduced upon exposure of polygonal cells to TGF-β (Fig. 5B). The growth factor also markedly reduced the expression of the two proteins at protein levels in a concentration-dependent manner (Fig. 5C), while phosphorylation of Smad2 was greatly increased in a concentration-dependent manner (Fig. 5D). These data suggest that even the normal phenotypes of primate CECs are prone to acquire fibroblastic phenotypes in response to TGF-β-stimulation.

Two distinct phenotypes of HCEC cultures and the use of TGF-β receptor inhibitor to block endothelial-mesenchymal transformation

The interesting findings observed in primate CECs led us to further study whether HCECs were subjected to the similar undesirable prerequisite cellular changes leading to endothelial-mesenchymal transformation. Of great interest, cultivated HCECs lost the characteristic contact-inhibited monolayer and polygonal phenotypes, and acquired fibroblastic cell morphology like primate CECs (Fig. 6A). However, consistent with the primate CECs when the CECs were cultivated with the specific inhibitor to the TGF-β receptor (SB431542), the inhibitor was able to block alteration of the cell shape to fibroblastic phenotypes. Similar to the inhibitory effect of SB431542 on fibroblastic phenotypes, both neutralizing antibody to TGF-β (Fig. 6B) and Smad3 inhibitor (Fig. 6C) also blocked cells from acquiring fibroblastic phenotypes. We then tested whether SB431542 was able to maintain endothelial function. The findings shown in Fig. 7A and Fig. 7B demonstrated that blocking the TGF-β receptor signaling enabled the subcellular localization of Na^+/K^+-ATPase and ZO-1 at the plasma membrane and their protein expression to be maintained. Of

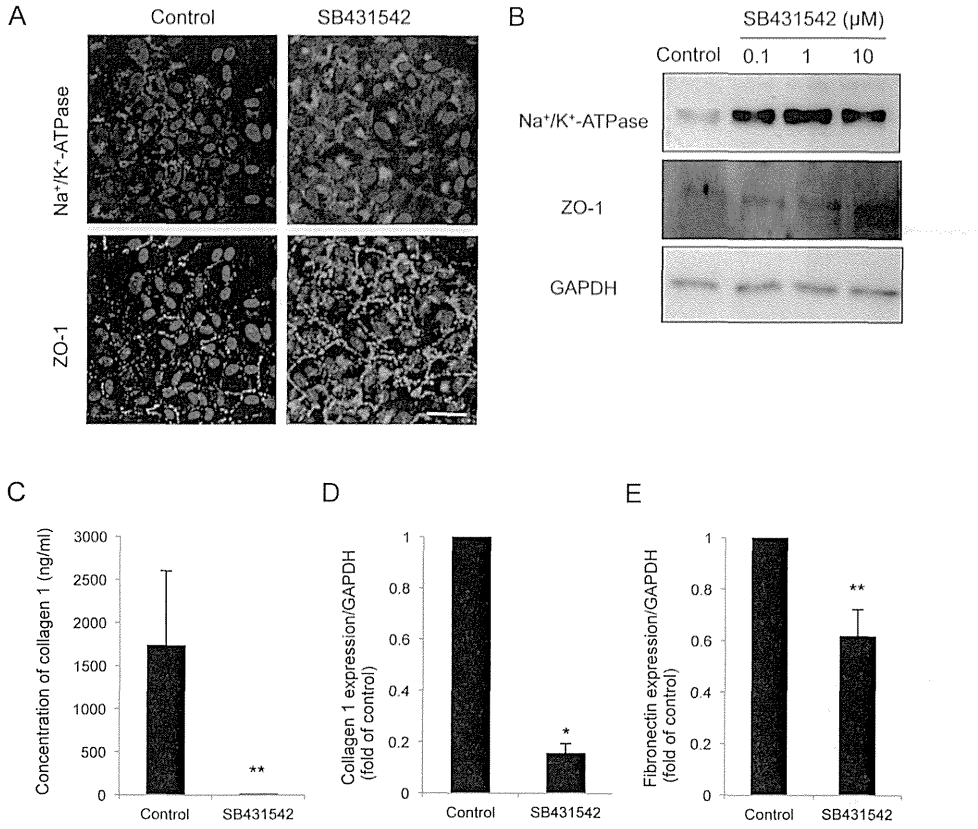

Figure 7. SB431542 maintained the functions and suppressed the fibroblastic change of HCECs. (A+B) Blocking the TGF-receptor signaling by SB431542 (A: 1 μM, B: 0.1, 1, and 10 μM) enabled the subcellular localization of Na^+/K^+-ATPase and ZO-1 at the plasma membrane and their protein expression to be maintained. Scale bar: 100 μm. (C) ELISA assay revealed that SB431542 significantly downregulated the secretion of type I collagen to the culture supernatant. **P<0.05. (D+E) Quantitative PCR showed that SB431542 significantly reduced the expression of type I collagen and fibronectin at the mRNA level. *$p<0.01$, ** $p<0.05$. Samples were prepared in duplicate. Immunoblotting, ELISA, and quantitative PCR were performed in duplicate.
doi:10.1371/journal.pone.0058000.g007

great importance, ELISA assay revealed that SB431542 markedly downregulated the secretion of type I collagen to the culture supernatant (Fig. 7C). Coincidentally, SB431542 markedly reduced the expression of type I collagen and fibronectin at the mRNA level (Fig. 7D, E).

Use of BMP-7 to suppress fibroblastic changes and maintain endothelial functions

Bone morphogenetic protein-7 (BMP-7) promotes MET and specifically inhibits the TGF-β-mediated epithelial-to-mesenchymal transition. Thus, that molecule has been used to antagonize the EMT process [31–34]. We therefore tested whether BMP-7 was able to antagonize the prerequisite changes of HCECs. The fibroblastic HCECs were treated with BMP-7 in a concentration ranging from 10 to 1000 ng/ml. Of important note, the elongated cell shapes of the fibroblastic phenotypes were reversed to the polygonal cell morphology in response to the presence of BMP-7 in a concentration-dependent manner (Fig. 8A). BMP-7 enabled the hexagonal cell morphology and actin cytoskeleton distribution at the cortex to be maintained (Fig. 8B), similar to that observed in normal CECs [35], and it also maintained the subcellular localization of Na^+/K^+-ATPase (Fig. 8C) and ZO-1 (Fig. 8D) at the plasma membrane. Thus, BMP-7 at the concentration of 1000 ng/ml was able to maintain CECs in polygonal and contact-inhibited phenotypes with a positive expression of function-related markers (Fig. 8E, F).

Discussion

Corneal endothelial dysfunction accompanied by visual disturbance is a major indication for corneal transplantation surgery [36,37]. Though corneal transplantation is widely performed for corneal endothelial dysfunction, researchers are currently seeking alternative methods to restore healthy corneal endothelium. The fact that corneal endothelium is cultured and stocked as 'master cells' from young donors allows for the transplantation of CECs with high functional ability and for an extended period of time. In addition, an HLA-matching transplantation to reduce the risk of rejection [38,39] and overcoming the shortage of donor corneas might be possible. Tissue bioengineering is a new approach to develop treatments for patients who have lost visual acuity [40]. To date, there are two methods that utilize bioengineering approaches: 1) use of cultured donor HCECs adhered on bioengineered constructs [4,5,7,9], and 2) transplantation of cultivated HCECs into the anterior chamber [11,41–43]. Regardless of which of the two methods is applied to clinical settings, establishment of an efficient cultivation technique for HCECs is essential and inevitable [44]. Many researchers have noticed that establishing a consistent long-term culture of HCECs is challenging [40]. Although the successful cultivation of HCECs has been reported by several groups, the procedures involved in the isolation and subsequent cultivation protocols varied greatly between laboratories [44]. One of the most difficult problems is

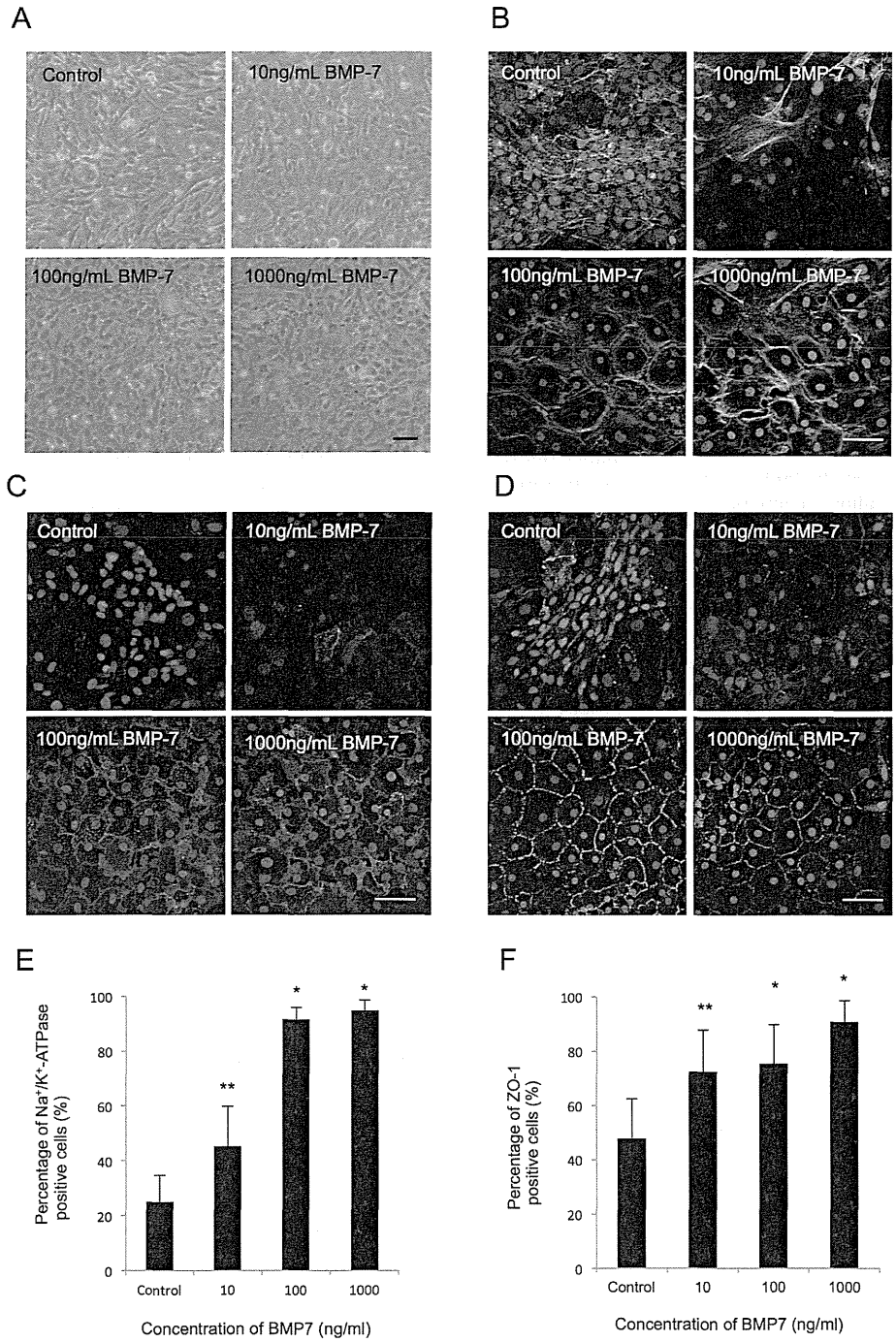

Figure 8. BMP7 suppressed fibroblastic change and maintained the functions of HCECs. (A) The elongated cell shapes of the fibroblastic phenotypes were reversed to a polygonal cell morphology in response to the presence of BMP-7 in a concentration-dependent manner. Scale bar: 50 μm. (B) BMP-7 enabled normal hexagonal cell morphology and actin cytoskeleton distribution at the cortex to be maintained. Scale bar: 100 μm. (C+D) BMP-7 maintained the subcellular localization of Na^+/K^+-ATPase and ZO-1at the plasma membrane. Scale bar: 100 μm. (E+F) The percentages of both Na^+/K^+-ATPase and ZO-1 positive cells treated with BMP-7 were significantly higher than in the control. * $p<0.01$, ** $p<0.05$. The experiment was performed in duplicate.
doi:10.1371/journal.pone.0058000.g008

that HCECs are vulnerable to undergoing massive fibroblastic change over each passage [40]. Therefore, it is essential to find means to circumvent the spontaneous transformation of the CECs in order to maintain the physiological phenotypes for the subsequent use for transplantation.

Transformation of endothelial cells to fibroblastic cells is designated as endothelial- mesenchymal transformation. Such transformation is triggered by TGF-β via the Smad2/3 pathway [16]. Endothelial-mesenchymal transformation causes the loss of the characteristic endothelial phenotypes, such as loss of the contact-inhibited monolayer and loss of the apical junctional

proteins at the plasma membrane. Furthermore, it causes induction of fibrillar proteins such as type I collagen and fibronectin. In this present study, we demonstrated that the fibroblastic phenotypes of cultivated CECs greatly lost the endothelial characteristics; expression of Na^+/K^+-ATPase and ZO-1 was markedly reduced and their subcellular localization was in the cytosol rather than the authentic plasma membrane location. Furthermore, fibroblastic phenotypes markedly enhance the production of fibrillar ECM proteins (type I collagen, fibronectin, and integrin α5) rather than basement membrane phenotypes (type IV and VIII collagens). The presence of such undesirable cells will greatly hamper the success of transplantation of cultivated cells in the clinical setting. Therefore, it is crucial to determine what causes the phenotypic changes and how to intervene in such endothelial-mesenchymal transformation processes of the cultivated CECs. The fact that phosphorylation of Smad2/3 was greatly enhanced in the fibroblastic phenotypes led us to conclude that the fibroblastic phenotypes in both primate and HCECs are mediated by TGF-β signaling. Therefore, we employed a specific inhibitor to the TGF-β receptor (SB431542) [45] to block the endothelial-mesenchymal transformation process observed in the fibroblastic phenotypes. SB431542 completely abolished the undesirable cellular changes, and when either primate or HCEC cultures were treated with SB431542, the prerequisite change of cells to fibroblastic phenotypes was completely abolished. Simultaneously, the characteristic subcellular location of ZO-1 and Na^+/K^+-ATPase is resumed at the plasma membrane and the expression of the two proteins is greatly increased at both mRNA and protein levels, suggesting that the barrier and pump functions in these cultures is intact. Moreover, we found that the production of fibrillar ECM proteins was greatly reduced. We further tested the effect of BMP-7, a well-known anti-EMT agent [31,34], to reverse the fibroblastic phenotypes of HCECs. BMP-7 also reversed the fibroblastic phenotypes to the normal endothelial cells with contact-inhibited monolayer and characteristic endothelial adhesion. Taken together, both SB431542 and BMP-7 can be powerful tools to maintain the normal endothelial phenotypes of the cultivated CECs, thus leading to a successful subsequent transplantation.

In conclusion, our findings showed that the use of the inhibitor to TGF-β receptor (SB431542) and/or anti-EMT molecules (BMP-7) enables HCECs to grow with maintaining normal physiological function (i.e., barrier and pump function). Although more extensive future studies would be beneficial, we have not observed any obvious adverse effects of continuous SB431542 or BMP-7 treatment on morphology and functions, even after several numbers of passages. This present study may prove to be the substantial protocol to provide the efficient *in vitro* expansion of HCECs. In addition, this novel strategy of inhibition of fibroblastic change during cultivation may ultimately provide clinicians with a new therapeutic modality in regenerative medicine, not only for the treatment of corneal endothelial dysfunctions, but also for a variety of pathological diseases in general.

Acknowledgments

The authors thank Dr. Morio Ueno, Dr. Michio Hagiya, Dr. Kiwamu Imagawa, Dr. Kenta Yamasaki, and Mr. Yuji Sakamoto for their valuable assistance with the experiments, and Mr. John Bush for reviewing the manuscript.

Author Contributions

Conceived and designed the experiments: NO EPK MN JH SK NK. Performed the experiments: NO MN. Analyzed the data: NO EPK MN JH SK NK. Contributed reagents/materials/analysis tools: NO SK NK. Wrote the paper: NO EPK NK.

References

1. Melles GR, Lander F, van Dooren BT, Pels E, Beekhuis WH (2000) Preliminary clinical results of posterior lamellar keratoplasty through a sclerocorneal pocket incision. Ophthalmology 107: 1850–1856; discussion 1857.
2. Price FW Jr, Price MO (2005) Descemet's stripping with endothelial keratoplasty in 50 eyes: a refractive neutral corneal transplant. J Refract Surg 21: 339–345.
3. Gorovoy MS (2006) Descemet-stripping automated endothelial keratoplasty. Cornea 25: 886–889.
4. Ishino Y, Sano Y, Nakamura T, Connon CJ, Rigby H, et al. (2004) Amniotic membrane as a carrier for cultivated human corneal endothelial cell transplantation. Invest Ophthalmol Vis Sci 45: 800–806.
5. Mimura T, Yamagami S, Yokoo S, Usui T, Tanaka K, et al. (2004) Cultured human corneal endothelial cell transplantation with a collagen sheet in a rabbit model. Invest Ophthalmol Vis Sci 45: 2992–2997.
6. Sumide T, Nishida K, Yamato M, Ide T, Hayashida Y, et al. (2006) Functional human corneal endothelial cell sheets harvested from temperature-responsive culture surfaces. FASEB J 20: 392–394.
7. Koizumi N, Sakamoto Y, Okumura N, Okahara N, Tsuchiya H, et al. (2007) Cultivated corneal endothelial cell sheet transplantation in a primate model. Invest Ophthalmol Vis Sci 48: 4519–4526.
8. Koizumi N, Sakamoto Y, Okumura N, Tsuchiya H, Torii R, et al. (2008) Cultivated corneal endothelial transplantation in a primate: possible future clinical application in corneal endothelial regenerative medicine. Cornea 27 Suppl 1: S48–55.
9. Koizumi N, Okumura N, Kinoshita S (2012) Development of new therapeutic modalities for corneal endothelial disease focused on the proliferation of corneal endothelial cells using animal models. Exp Eye Res 95: 60–67.
10. Okumura N, Ueno M, Koizumi N, Sakamoto Y, Hirata K, et al. (2009) Enhancement on primate corneal endothelial cell survival in vitro by a ROCK inhibitor. Invest Ophthalmol Vis Sci 50: 3680–3687.
11. Okumura N, Koizumi N, Ueno M, Sakamoto Y, Takahashi H, et al. (2012) ROCK inhibitor converts corneal endothelial cells into a phenotype capable of regenerating in vivo endothelial tissue. Am J Pathol 181: 268–277.
12. Miyata K, Drake J, Osakabe Y, Hosokawa Y, Hwang D, et al. (2001) Effect of donor age on morphologic variation of cultured human corneal endothelial cells. Cornea 20: 59–63.
13. Joyce NC, Zhu CC (2004) Human corneal endothelial cell proliferation: potential for use in regenerative medicine. Cornea 23: S8–S19.
14. Zavadil J, Bottinger EP (2005) TGF-beta and epithelial-to-mesenchymal transitions. Oncogene 24: 5764–5774.
15. Wendt MK, Allington TM, Schiemann WP (2009) Mechanisms of the epithelial-mesenchymal transition by TGF-beta. Future Oncol 5: 1145–1168.
16. Saika S (2006) TGFbeta pathobiology in the eye. Lab Invest 86: 106–115.
17. Kaimori A, Potter J, Kaimori JY, Wang C, Mezey E, et al. (2007) Transforming growth factor-beta1 induces an epithelial-to-mesenchymal transition state in mouse hepatocytes in vitro. J Biol Chem 282: 22089–22101.
18. Chen KH, Harris DL, Joyce NC (1999) TGF-beta2 in aqueous humor suppresses S-phase entry in cultured corneal endothelial cells. Invest Ophthalmol Vis Sci 40: 2513–2519.
19. Kim TY, Kim WI, Smith RE, Kay ED (2001) Role of p27(Kip1) in cAMP- and TGF-beta2-mediated antiproliferation in rabbit corneal endothelial cells. Invest Ophthalmol Vis Sci 42: 3142–3149.
20. Naumann GO, Schlotzer-Schrehardt U (2000) Keratopathy in pseudoexfoliation syndrome as a cause of corneal endothelial decompensation: a clinicopathologic study. Ophthalmology 107: 1111–1124.
21. Kawaguchi R, Saika S, Wakayama M, Ooshima A, Ohnishi Y, et al. (2001) Extracellular matrix components in a case of retrocorneal membrane associated with syphilitic interstitial keratitis. Cornea 20: 100–103.
22. Koizumi N, Suzuki T, Uno T, Chihara H, Shiraishi A, et al. (2008) Cytomegalovirus as an etiologic factor in corneal endotheliitis. Ophthalmology 115: 292–297 e293.
23. Song JS, Lee JG, Kay EP (2010) Induction of FGF-2 synthesis by IL-1beta in aqueous humor through P13-kinase and p38 in rabbit corneal endothelium. Invest Ophthalmol Vis Sci 51: 822–829.
24. Li W, Sabater AL, Chen YT, Hayashida Y, Chen SY, et al. (2007) A novel method of isolation, preservation, and expansion of human corneal endothelial cells. Invest Ophthalmol Vis Sci 48: 614–620.
25. Zhu C, Joyce NC (2004) Proliferative response of corneal endothelial cells from young and older donors. Invest Ophthalmol Vis Sci 45: 1743–1751.
26. Rheinwald JG, Green H (1975) Serial cultivation of strains of human epidermal keratinocytes: the formation of keratinizing colonies from single cells. Cell 6: 331–343.
27. Koizumi N, Fullwood NJ, Bairaktaris G, Inatomi T, Kinoshita S, et al. (2000) Cultivation of corneal epithelial cells on intact and denuded human amniotic membrane. Invest Ophthalmol Vis Sci 41: 2506–2513.

28. Ko MK, Kay EP (2001) Subcellular localization of procollagen I and prolyl 4-hydroxylase in corneal endothelial cells. Exp Cell Res 264: 363–371.
29. Parsons CJ, Takashima M, Rippe RA (2007) Molecular mechanisms of hepatic fibrogenesis. J Gastroenterol Hepatol 22 Suppl 1: S79–84.
30. Ma FY, Sachchithananthan M, Flanc RS, Nikolic-Paterson DJ (2009) Mitogen activated protein kinases in renal fibrosis. Front Biosci (Schol Ed) 1: 171–187.
31. Zeisberg M, Hanai J, Sugimoto H, Mammoto T, Charytan D, et al. (2003) BMP-7 counteracts TGF-beta1-induced epithelial-to-mesenchymal transition and reverses chronic renal injury. Nat Med 9: 964–968.
32. Simic P, Vukicevic S (2007) Bone morphogenetic proteins: from developmental signals to tissue regeneration. Conference on bone morphogenetic proteins. EMBO Rep 8: 327–331.
33. Buijs JT, Rentsch CA, van der Horst G, van Overveld PG, Wetterwald A, et al. (2007) BMP7, a putative regulator of epithelial homeostasis in the human prostate, is a potent inhibitor of prostate cancer bone metastasis in vivo. Am J Pathol 171: 1047–1057.
34. Zeisberg M, Yang C, Martino M, Duncan MB, Rieder F, et al. (2007) Fibroblasts derive from hepatocytes in liver fibrosis via epithelial to mesenchymal transition. J Biol Chem 282: 23337–23347.
35. Barry PA, Petroll WM, Andrews PM, Cavanagh HD, Jester JV (1995) The spatial organization of corneal endothelial cytoskeletal proteins and their relationship to the apical junctional complex. Invest Ophthalmol Vis Sci 36: 1115–1124.
36. Darlington JK, Adrean SD, Schwab IR (2006) Trends of penetrating keratoplasty in the United States from 1980 to 2004. Ophthalmology 113: 2171–2175.
37. Price MO, Price FW Jr. (2010) Endothelial keratoplasty – a review. Clin Experiment Ophthalmol 38: 128–140.
38. Khaireddin R, Wachtlin J, Hopfenmuller W, Hoffmann F (2003) HLA-A, HLA-B and HLA-DR matching reduces the rate of corneal allograft rejection. Graefes Arch Clin Exp Ophthalmol 241: 1020–1028.
39. Coster DJ, Williams KA (2005) The impact of corneal allograft rejection on the long-term outcome of corneal transplantation. Am J Ophthalmol 140: 1112–1122.
40. Engelmann K, Bednarz J, Valtink M (2004) Prospects for endothelial transplantation. Exp Eye Res 78: 573–578.
41. Mimura T, Shimomura N, Usui T, Noda Y, Kaji Y, et al. (2003) Magnetic attraction of iron-endocytosed corneal endothelial cells to Descemet's membrane. Exp Eye Res 76: 745–751.
42. Mimura T, Yamagami S, Yokoo S, Yanagi Y, Usui T, et al. (2005) Sphere therapy for corneal endothelium deficiency in a rabbit model. Invest Ophthalmol Vis Sci 46: 3128–3135.
43. Patel SV, Bachman LA, Hann CR, Bahler CK, Fautsch MP (2009) Human corneal endothelial cell transplantation in a human ex vivo model. Invest Ophthalmol Vis Sci 50: 2123–2131.
44. Peh GS, Beuerman RW, Colman A, Tan DT, Mehta JS (2011) Human corneal endothelial cell expansion for corneal endothelium transplantation: an overview. Transplantation 91: 811–819.
45. Inman GJ, Nicolas FJ, Callahan JF, Harling JD, Gaster LM, et al. (2002) SB-431542 is a potent and specific inhibitor of transforming growth factor-beta superfamily type I activin receptor-like kinase (ALK) receptors ALK4, ALK5, and ALK7. Mol Pharmacol 62: 65–74.

Acta Ophthalmologica

Letter to the Editor

Relationship between frequent swimming pool use and lacrimal duct obstruction

Akihide Watanabe,[1] Eri Kondoh,[1] Dinesh Selva,[2] Kojiro Imai,[1] Koichi Wakimasu,[1] Biji Araki[1] and Shigeru Kinoshita[1]

[1]Department of Ophthalmology, Kyoto Prefectural University of Medicine, Kyoto, Japan; [2]Discipline of Ophthalmology and Visual Sciences, South Australian Institute of Ophthalmology and Royal Adelaide Hospital, Adelaide, SA, Australia

doi: 10.1111/aos.12273

Editor,

In our clinical practice, we often encounter frequent swimming pool users and swimming instructors to be among patients with acquired lacrimal duct obstruction (LDO). Only one previous report of 45 patients with primary acquired nasolacrimal duct obstruction has noted that history of swimming pool exposure may be associated with the development of LDO (Ohtomo et al. 2013). To examine whether or not frequent swimming pool use is associated with LDO, we conducted a questionnaire survey of patients who underwent treatment for LDO and compared the results with an age- and gender-matched control group.

The questionnaire survey was conducted in 332 patients who visited the Department of Ophthalmology at Kyoto Prefectural University of Medicine, Kyoto, Japan, and underwent surgical treatment (dacryocystorhinostomy or silicone tube insertion) for LDO between April 2003 and March 2009. LDO was defined as the complete obstruction of the nasolacrimal duct, canaliculus or both by syringing and probing during surgery. A questionnaire survey on the frequency of swimming pool use was given to 332 LDO patients, of whom 227 completed the questionnaire (adopted LDO group; 68.4%, 45 males and 182 females, mean age: 65.4 ± 12.8 years), and a control group of 625 patients without LDO (159 males and 466 females, mean age: 63.3 ± 15.3 years), recruited from the outpatient clinic and matched for age and gender. Statistical analysis was performed on the correlation between LDO and frequency of swimming pool use and the frequency between the two groups. Frequent swimming pool use was defined as the use of the pool one or more times per month for a period of at least 6 months. Individuals who had onset of symptoms prior to commencing swimming pool use were not defined as frequent users. Individuals unable to use swimming pools for medical reasons were excluded from the study.

Table 1. Percentage of frequent swimming pool use.

Frequent swimming pool use yes or no, *n* (%)	Adopted LDO group (*n* = 227)	Control group (*n* = 625)
Yes	35 (15.4%)***	20 (3.2%)***
Mean age (SD), years	60.1 (15.9)*	64.7 (12.3)
Range	18–86	30–88
Men	7 (20.0%)	4 (20.0%)
Women	28 (80.0%)	16 (80.0%)
No	192 (84.6%)	605 (96.8%)
Mean age (SD), years	66.4 (11.9)*	63.2 (15.4)
Range	21–87	11–89
Men	38 (19.8%)	155 (25.6%)
Women	154 (80.2%)	450 (74.4%)

LDO = lacrimal duct obstruction, SD = standard deviation.
* $p < 0.05$, *** $p < 0.0001$ (Chi square test).

The percentage of frequent swimming pool use differed significantly and statistically between the LDO group (35 of 227 patients, 15.4%) and the control group (20 of 625 subjects, 3.2%). In the LDO group, the average age of patients with frequent swimming pool use (60.1 years old) significantly differed from the patients without frequent use (66.4) (Table 1). In the LDO group, patient-age-related percentages of frequent swimming pool use were 100% (2/2, ages 10–19), 20% (1/5, ages 20–29), 0% (0/4, ages 30–39), 40% (4/10, ages 40–49), 18.9% (7/37, ages 50–59), 18.4% (14/76, ages 60–69), 7% (5/71, ages 70–79) and 9% (2/22, ages 80–89).

Previous studies have reported epidemiological evidence that bathing or swimming in polluted waters is a potential health risk (Seyfried et al. 1985). In most swimming pools, microbiological control is performed by disinfection via the addition of chlorine. The disinfection properties of free chlorine are linked to its oxidant capacity, and chlorination of swimming pool water leads to the formation of disinfection by-products, including combined chlorine or trihalomethanes, which are associated with some types of illness (Florentin et al. 2011). The phenomenon of a swimming-induced rhinitis in elite swimmers in chlorinated pools has been reported (Alves et al. 2010), and allergic rhinitis may have a role in primary acquired LDO (Eriman et al. 2012). Thus, it is possible that combined chlorine in water is one of the factors potentially involved in LDO among swimming pool users, and our results suggest that frequent swimming pool use may be a risk factor for LDO. Further investigation is needed to provide a more detailed analysis of the relationship between LDO and the quality of swimming pool water.

References

Alves A, Martins C & Delgado L (2010): Exercise-induced rhinitis in competitive swimmers. Am J Rhinol Allergy **24**: 114–117.

Eriman M, Kinis V, Habesoglu M et al. (2012): Role of allergy in primary acquired nasolacrimal duct obstruction. J Craniofac Surg **23**: 1620–1623.

Florentin A, Hautemanière A & Hartemann P (2011): Health effects of disinfection by-products in chlorinated swimming pools. Int J Hyg Environ Health **214**: 461–469.

Ohtomo K, Ueta T, Toyama T & Nagahara M (2013): Predisposing factors for primary acquired nasolacrimal duct obstruction. Graefes Arch Clin Exp Ophthalmol **251**: 1835–1839.

Seyfried PL, Tobin RS, Brown NE & Ness PF (1985): A prospective study of swimming-related illness. I. Swimming-associated health risk. Am J Public Health **75**: 1068–1070.

Correspondence:
Akihide Watanabe, MD
Department of Ophthalmology
Kyoto Prefectural University of Medicine
465 Kajii-cho
Kamigyo-ku
Kyoto 602-0841, Japan
Tel: + 81 75 251 5578
Fax: + 81 75 251 5663
Email: awatanab@koto.kpu-m.ac.jp

Involvement of Cyclin D and p27 in Cell Proliferation Mediated by ROCK Inhibitors Y-27632 and Y-39983 During Corneal Endothelium Wound Healing

Naoki Okumura,[1,2] Shinichiro Nakano,[1] EunDuck P. Kay,[1] Ryohei Numata,[1] Aya Ota,[1] Yoshihiro Sowa,[3] Toshiyuki Sakai,[3] Morio Ueno,[2] Shigeru Kinoshita,[2] and Noriko Koizumi[1]

[1]Department of Biomedical Engineering, Faculty of Life and Medical Sciences, Doshisha University, Kyotanabe, Japan
[2]Department of Ophthalmology, Kyoto Prefectural University of Medicine, Kyoto, Japan
[3]Department of Molecular-Targeting Cancer Prevention, Kyoto Prefectural University of Medicine, Kyoto, Japan

Correspondence: Noriko Koizumi, Department of Biomedical Engineering, Faculty of Life and Medical Sciences, Doshisha University, Kyotanabe 610-0321, Japan; nkoizumi@mail.doshisha.ac.jp.

Submitted: April 14, 2013
Accepted: September 26, 2013

Citation: Okumura N, Nakano S, Kay EP, et al. Involvement of cyclin D and p27 in cell proliferation mediated by ROCK inhibitors Y-27632 and Y-39983 during corneal endothelium wound healing. *Invest Ophthalmol Vis Sci.* 2014;55:318–329. DOI: 10.1167/iovs.13-12225

Purpose. To investigate the molecular mechanism of Rho-associated kinase (ROCK) inhibitors Y-27632 and Y-39983 on corneal endothelial cell (CEC) proliferation and their wound-healing effect.

Methods. The expression of G_1 proteins of the cell cycle and expression of phosphorylated Akt in monkey CECs (MCECs) treated with Y-27632 were determined by Western blotting. The effect of Y-39983 on the proliferation of MCECs and human CECs (HCECs) was evaluated by both Ki67 staining and incorporation of BrdU. As an in vivo study, Y-39983 was topically instilled in a corneal-endothelial partially injured rabbit model, and CEC proliferation was then evaluated.

Results. Investigation of the molecular mechanism of Y-27632 on CEC proliferation revealed that Y-27632 facilitated degradation of p27Kip1 (p27), and promoted the expression of cyclin D. When CECs were stimulated with Y-27632, a 1.7-fold increase in the activation of Akt was seen in comparison to the control after 1 hour. The presence of LY294002, the PI 3-kinase inhibitor, sustained the level of p27. When the efficacy of Y-39983 on cell proliferation was measured in a rabbit model, Y-39983 eye-drop instillation demonstrated rapid wound healing in a concentration range of 0.095 to 0.95 mM, whereas Y-27632 demonstrated rapid wound healing in a concentration range of 3 to 10 mM.

Conclusions. These findings show that ROCK inhibitors employ both cyclin D and p27 via PI 3-kinase signaling to promote CEC proliferation, and that Y-39983 may be a more potent agent than Y-27632 for facilitating corneal endothelium wound healing.

Keywords: corneal endothelial cells, ROCK inhibitor, bullous keratopathy, cell proliferation

It is well known that healthy corneal endothelium is vital for maintaining homeostatic corneal transparency and clear vision.[1] To date, full-thickness corneal transplantation or endothelial keratoplasty have been the only therapeutic choices available for the restoration of clear vision lost due to endothelial disorders.[2] In fact, more than 40,000 corneal transplantations were performed in 2011 in the United States alone.[2] In both 2009 and 2010, more than 40% of the corneal transplantation surgeries performed worldwide were endothelial keratoplasty,[2] thus suggesting that the primary disorder requiring corneal grafting is corneal endothelial dysfunction. Despite the high incidence of endothelial keratoplasty surgeries being performed, problems associated with corneal transplantation, such as allograft rejection, primary graft failure, and continuous loss of cell density, have yet to be resolved.[2–4]

As an alternative to corneal transplantation, transplantations of cultivated human corneal endothelial cells (HCECs) by a tissue engineering technique[5–10] or drug therapies[11–13] are expected to provide new therapeutic pathways for the treatment of corneal endothelial dysfunction. The applications of those two therapeutic approaches, as well as the purposes for which they are specifically intended, are distinct from one another (i.e., drug therapy may be a powerful tool in cases of early-stage corneal endothelial dysfunction in which stem cells or progenitor cells[14,15] are still maintained in the tissue, whereas transplantation of cultivated HCECs may be useful for the treatment of a fully progressed corneal endothelial dysfunction).[13]

In our previous study, we demonstrated that Y-27632, a specific Rho-associated kinase (ROCK), increased the proliferative potential of cultivated primate CECs in vitro.[16] We also reported that the topical administration of ROCK inhibitor Y-27632 enhanced corneal endothelial wound healing in an in vivo rabbit model, as the inhibitor facilitated cell proliferation as one of the major mechanisms.[11] In addition, we recently reported that the administration of ROCK-inhibitor Y-27632 eye drops recovers corneal clarity and thickness, especially in some patients with focal-edema-type Fuchs' corneal dystrophy.[12,13] Surprisingly, the best-corrected visual acuity of one bullous keratopathy patient that we reported recovered from logMAR 0.7 to –0.18, and with a completely transparent cornea, thus prompting us to cancel a corneal transplantation that was previously scheduled for that patient.[12]

In this present study, we investigated the molecular mechanism by which ROCK inhibitor Y-27632 stimulates the proliferation of CECs. Our results show that Y-27632 employs phosphatidylinositol 3-kinase (PI 3-kinase) signaling that subsequently regulates two proteins of the G_1 phase of the cell cycle: upregulation of cyclin D, and downregulation of p27Kip1 (p27); both activities being required for G_1/S progression. In addition, we investigated the novel, selective ROCK inhibitor Y-39983, an inhibitor with a reportedly higher potency than Y-27632 for inhibiting ROCK activity.[17,18] We then compared Y-27632 and Y-39983 with regard to their action on the proliferation of CECs, both in vitro and in vivo. We found that a lower concentration of Y-39983 (0.3 μM or 3.0 μM) stimulates the proliferation of CECs to the same level stimulated by 10 μM of Y-27632. Furthermore, our findings demonstrated that the topical administration of Y-39983 enhances corneal endothelial wound healing associated with cell proliferation in an in vivo rabbit model. Those results suggest that Y-39983 may be a highly effective drug candidate for the treatment of corneal endothelial dysfunction.

Materials and Methods

Materials

FNC Coating Mix was purchased from Athena Environmental Sciences, Inc. (Baltimore, MD). Collagenase A was purchased from Roche Applied Science (Penzberg, Germany). Dulbecco's modified Eagle's medium, fibroblast growth factor 2 (FGF-2), Trypsin-EDTA, OptiMEM-I, Alexa Fluor 488-conjugated goat anti-mouse IgG, and Click-iT EdU Imaging Kits were purchased from Life Technologies Corp. (Carlsbad, CA). Y-27632, LY-294002, chondroitin sulfate, and Alizarin red S were purchased from Wako Pure Chemical Industries, Ltd. (Osaka, Japan). Epidermal growth factor (EGF), ascorbic acid, calcium chloride, anti-mouse Ki67 antibody, and Phosphatase Inhibitor Cocktail 2 were purchased from Sigma-Aldrich Co. (St. Louis, MO). The 4′,6-diamidino-2-phenylindole (DAPI) was purchased from Vector Laboratories (Burlingame, CA); CellTiter-Glo Luminescent Cell Viability Assay was purchased from Promega Corporation (Madison, WI); Cell Proliferation Biotrak ELISA System, version 2 was purchased from GE Healthcare Life Sciences (Buckinghamshire, England); BrdU labeling solution was purchased from Amersham Biosciences (Freiburg, Germany); and RIPA buffer was purchased from Bio-Rad Laboratories (Hercules, CA).

Protease Inhibitor Cocktail was purchased from Nacalai Tesque (Kyoto, Japan). Nonfat dry milk, Cyclin D1, Cyclin D3, Akt1, phosphorylated Akt, and horseradish peroxidase-conjugated secondary antibodies were purchased from Cell Signaling Technology, Inc. (Danvers, MA). Cdc25A and p27 were purchased from Santa Cruz Biotechnology (Santa Cruz, CA). Glyceraldehyde 3-phosphate dehydrogenase (GAPDH) was purchased from Abcam (Cambridge, UK).

Animal Experiment Approval

In all experiments, animals were housed and treated in accordance with the ARVO Statement for the Use of Animals in Ophthalmic and Vision Research. The rabbit experiments were performed at Doshisha University (Kyoto, Japan) according to the protocol approved by the Animal Care and Use Committee (Approval No. 1224) of the university. The human tissue used in this study was handled in accordance with the tenets set forth in the Declaration of Helsinki. For all eye donations from deceased donors, written consent to use the eyes for research was obtained from the next of kin. All donor tissue was obtained under the tenets of the Uniform Anatomical Gift Act (UAGA) of the particular state where both the donor consent and tissue were obtained.

Cell Culture of Monkey CECs

CECs used to produce the monkey CEC (MCEC) culture were obtained from eight corneas of four cynomolgus monkeys (3 to 5 years of age; estimated equivalent human age: 5 to 20 years), respectively housed at Nissei Bilis and the Keari Co., Ltd., Osaka, Japan. The MCECs were cultivated in a modified protocol as described previously.[9,16,19] Briefly, Descemet's membrane, including corneal endothelium, was stripped and digested at 37°C for 2 hours with 1 mg/mL collagenase A. After digestion, the MCECs were resuspended in culture medium and plated in one well of a six-well plate coated with FNC Coating Mix. All primary cell cultures and serial passages of the MCECs were performed in growth medium composed of Dulbecco's modified Eagle's medium supplemented with 10% fetal bovine serum (FBS), 50 U/mL penicillin, 50 μg/mL streptomycin, and 2 ng/mL FGF-2. The cells were then cultured in a humidified atmosphere at 37°C in 5% CO_2, with the culture medium being changed every 2 days. The MCECs were then trypsinized with 0.05% Trypsin-EDTA for 5 minutes at 37°C, and passaged at the ratio of 1:2 to 4 once they had reached confluence. Cultivated MCECs at passages 2 through 5 were used for all experiments. Y-27632 (a selective inhibitor of Rho kinase) and LY-294002 (a PI 3-kinase inhibitor) were tested for their cell proliferation and antiproliferation effects. In addition, ROCK-inhibitor Y-39983 (obtained from Mitsubishi Pharma Corporation, Osaka, Japan) was tested for its effect on cell proliferation.

Cell Culture of HCECs. The HCECs were cultivated using the recently reported protocol.[13] Briefly, Descemet's membrane, including CECs, was stripped and digested with 1 mg/mL collagenase A, and the HCECs were then resuspended in culture medium. The culture medium was prepared from basal medium after conditioning by inactivated NIH-3T3 fibroblasts. The inactivated NIH-3T3 was maintained by basal medium for 24 hours. Then, the medium was collected, filtered, and used as the culture medium for the HCECs. Basal medium was composed of OptiMEM-I supplemented with 8% FBS, 5 ng/mL EGF, 20 μg/mL ascorbic acid, 200 mg/L calcium chloride, 0.08% chondroitin sulfate, and 50 μg/mL gentamicin. Inactivation of the 3T3 fibroblasts was performed as described previously.[20,21] The HCECs were cultured in a humidified atmosphere at 37°C in 5% CO_2, with the culture medium being changed every 2 days. Cultivated HCECs at passages 2 through 5 were used for all experiments.

In Vitro Wound Healing Assay

The MCECs were further maintained in culture for 14 days after reaching confluence so as to form a contact-inhibited hexagonal layer. Scrape wounds were then produced using a plastic pipette tip to create six linear defect sites in each culture dish. The culture medium was then replaced with fresh medium containing 10 μM of Y-27632, while control cells were maintained in the absence of Y-27632. The percentage of Ki67-positive ($Ki67^+$) cells among the proliferating and migrating cells in the wounded area was determined after 48 hours of incubation. All experiments were performed in duplicate.

In Vivo Wound Healing After Y-27632 Treatment

As an in vivo wound model, the corneal endothelium of nine Japanese white rabbits was damaged in a modified protocol as described previously.[11,22,23] Briefly, a stainless-steel 7-mm-

diameter probe was immersed in liquid nitrogen for 3 minutes to stabilize its temperature at approximately −196°C, and the probe was then placed onto the rabbit cornea for 15 seconds under general anesthesia. Care was taken to confirm that this procedure did not induce complete blindness or any severe general adverse effect. Next, 1, 3, or 10 mM of Y-27632 diluted in PBS (50 μL) was topically instilled in eye eye of each rabbit six times daily, while PBS alone was instilled in the fellow eye of each rabbit as a control. After 48 hours of treatment, the rabbits were euthanized and the $Ki67^+$ cells located at the edge of the original corneal endothelium wound (3.5-mm distant from the center of the cornea) were then evaluated.

In Vivo Wound Healing After Y-39983 Treatment

The corneal endothelium of 27 Japanese white rabbits was damaged by transcorneal freezing as described above. Next, 0.095 mM (0.003%), 0.32 mM (0.01%), or 0.95 mM (0.03%) of Y-39983 diluted in PBS (50 μL) was topically instilled in one eye of each rabbit six times daily, while PBS alone was instilled in the fellow eye of each rabbit as a control. After 48 hours of treatment, the anterior segment of each eye was assessed by use of a slit-lamp microscope and the rabbits were then euthanized. The corneal endothelium wound area was then evaluated by use of Alizarin red staining after enucleation. Briefly, corneas were stained with 0.5% Alizarin red for 1 minute, fixed in 4% formaldehyde, and then examined under a fluorescence microscope (BZ-9000; Keyence, Osaka, Japan). The residual wound areas shown in the Alizarin red staining images were then evaluated by use of Image J (National Institutes of Health, Bethesda, MD) software. In addition, $Ki67^+$ cells located at the edge of the original corneal endothelium wound in the same specimens were evaluated.

Ki67 Immunostaining

MCECs or HCECs cultured on Lab-Tek Chamber Slides (NUNC A/S, Roskilde, Denmark), or flat-mounted whole corneal specimens, were fixed in 4% formaldehyde for 10 minutes at room temperature (RT), and then incubated for 30 minutes with 1% bovine serum albumin (BSA). To investigate the proliferation of the CECs, immunohistochemical analyses of Ki67 staining was performed. Samples were incubated with a 1:400 dilution of anti-mouse Ki67 antibody overnight at 4°C, washed three times in PBS, and then incubated with a 1:2000 dilution of Alexa Fluor 488-conjugated goat anti-mouse IgG for 2 hours at RT. Cell nuclei were stained with DAPI. The slides were then examined under a fluorescence microscope (TCS SP2 AOBS; Leica Microsystems, Wetzlar, Germany).

Effect of Y-39983 on the MCECs in Culture

MCECs were seeded at a density of 5.0×10^3 cells/cm^2 per well on a 96-well plate for 24 hours, and then subjected to serum starvation for an additional 24 hours in the presence or absence of Y-39983 (0.03 μM, 0.3 μM, and 3.0 μM). The MCECs were then examined under a phase-contrast microscope (Leica), and the number of viable cells was determined by use of the CellTiter-Glo Luminescent Cell Viability Assay performed in accordance with the manufacturer's recommended protocol. The number of MCECs at 24 hours after stimulation with Y-39983 was measured by use of the Veritas Microplate Luminometer (Promega). Five samples were prepared for each group.

EdU-Labeling Assay

MCECs seeded at a density of 5.0×10^4 cells/cm^2 on micro cover glass (Matsunami Glass Ind., Ltd., Osaka, Japan) in a 24-well plate were maintained for 24 hours, and then incubated in the absence of serum for an additional 24 hours with or without Y-39983 (0.03 μM, 0.3 μM, and 3.0 μM). DNA synthesis was determined by use of Click-iT EdU Imaging Kits using the recommended protocol. Briefly, the cells were incubated for an additional 24 hours with a 20 μM EdU-labeling reagent. The cells were then washed in PBS, fixed with 4% formaldehyde for 20 minutes at RT, and washed with 3% BSA. The cells were then incubated for 30 minutes at RT with a Click-iT reaction cocktail, washed 3 times in PBS, and mounted on glass slides with anti-fading mounting medium containing DAPI. The slides were then examined under the TCS SP2 AOBS fluorescence microscope.

BrdU ELISA

MCECs or HCECs were seeded at the density of 5000 cells per well in a 96-well plate for 24 hours, and then incubated in the absence of serum for an additional 24 hours in the presence or absence of Y-39983 ($n = 5$). DNA synthesis was detected as incorporation of 5-bromo-2′-deoxyuridine (BrdU) into the Cell Proliferation Biotrak ELISA system, version 2, according to the manufacturer's instructions. Briefly, MCECs or HCECs were incubated with 10 mol/L BrdU for 24 hours in a humidified atmosphere at 37°C in 5% CO_2. The cultured cells were incubated with 10 μM BrdU labeling solution for 2 hours, and then incubated with 100 μL of monoclonal antibody against BrdU for 30 minutes. The BrdU absorbance was measured directly using a spectrophotometric microplate reader (Promega) at a test wavelength of 450 nm.

Immunoblotting

The MCECs were washed with ice-cold PBS, and then lysed with ice-cold RIPA buffer containing Phosphatase Inhibitor Cocktail 2 and Protease Inhibitor Cocktail. The lysates were centrifuged at 15,000 rpm for 10 minutes at 4°C to sediment the cell debris. The supernatant representing total proteins was collected and the protein concentration of the sample was assessed by use of the BCA Protein Assay Kit (Takara Bio, Inc., Otsu, Japan). An equal amount of protein was fractionated by SDS-PAGE; proteins were transferred to polyvinylidene difluoride (PVDF) membranes. The membranes were then blocked with 3% nonfat dry milk in TBS-T buffer (50 mM Tris, pH 7.5, 150 mM $NaCl_2$, and 0.1% Tween20) for 1 hour at RT, followed by an overnight incubation at 4°C with the following primary antibodies: Cdc25A (1:1000), Cyclin D1 (1:1000), Cyclin D3 (1:1000), p27 (1:1000), Akt1 (1:2000), phosphorylated Akt (1:2000), and GAPDH (1:3000). The blots were washed, and then incubated with horseradish peroxidase-conjugated secondary antibodies (1:5000). The blots were then developed with luminal for enhanced chemiluminescence using the ECL Advanced Western Blotting Detection Kit (GE Healthcare, Piscataway, NJ), documented using an LAS4000S (Fuji Film, Tokyo, Japan) cooled charge-coupled-device camera gel documentation system, and analyzed with Image J software.

Statistical Analysis

The statistical significance (P value) in mean values of the two-sample comparison was determined with the Student's t-test. The statistical significance in the comparison of multiple sample sets was analyzed by use of the Dunnett's multiple-comparisons test. Values shown on the graphs represent the mean ± SEM.

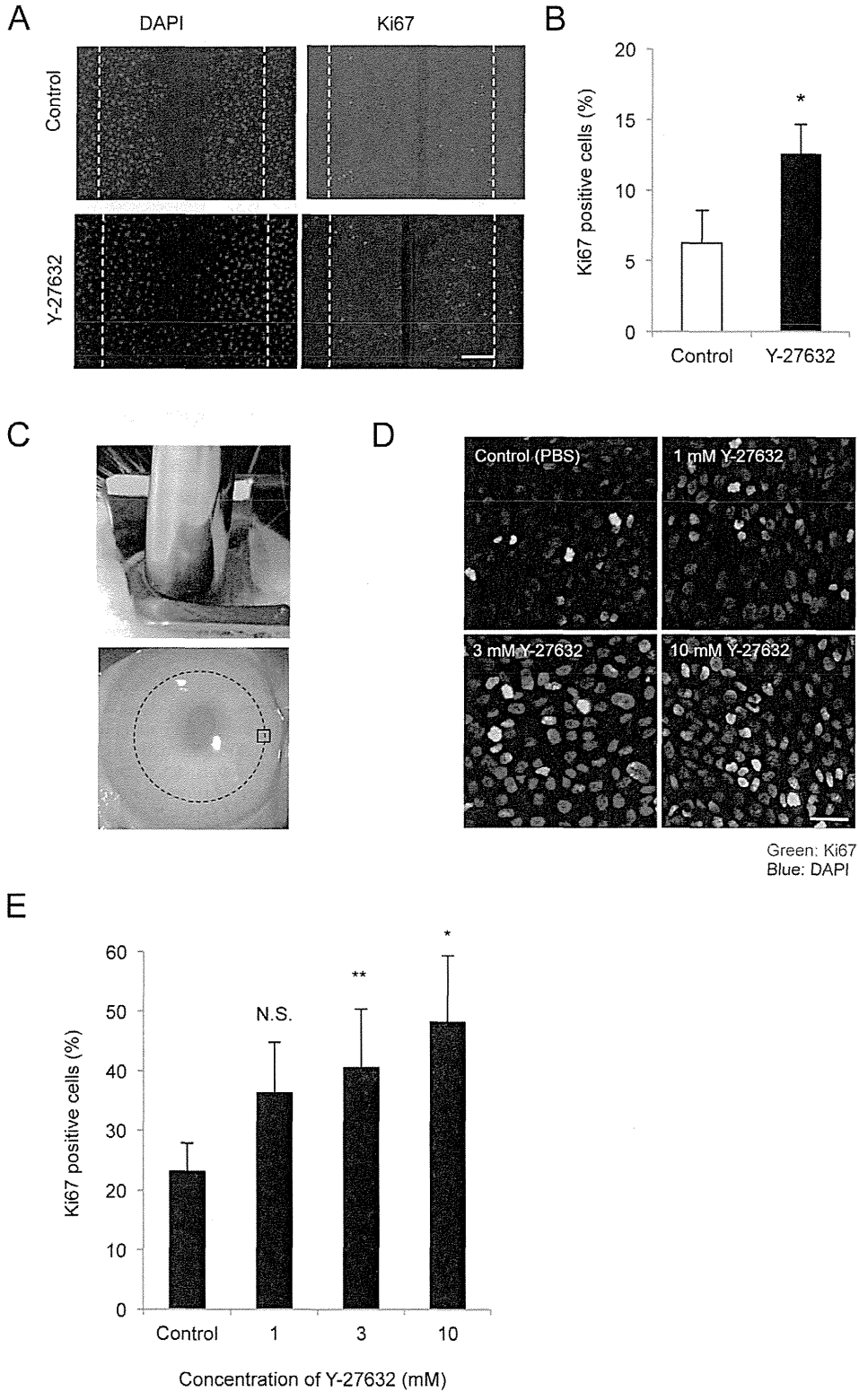

Figure 1. Effect of ROCK-inhibitor Y-27632 on cell proliferation during in vitro and in vivo wound healing. (**A**) Effect of Y-27632 on the proliferation of cultured MCECs. Representative Ki67 staining images obtained 48 hours after scrape wounding treated with 10 μM Y-27632. *Scale bar*: 500 μm. (**B**) In the absence of Y-27632, approximately 6% of the cell population in the injury sites was found to be composed of $Ki67^+$ cells. However, in the cells treated with Y-27632, 13% of the cells in the injury site were $Ki67^+$ cells. The $Ki67^+$ cells were counted in the wounded area ($n = 4$). The images are representative of two independent experiments. (**C**) Central rabbit corneal endothelium was partially damaged by transcorneal cryogenic injury. *Dotted line*: original wounded area; *solid line*: edge of the original wounded area. Y-27632 (50 μL) was topically applied in one eye of each animal six times daily for 2 days. (**D**, **E**) $Ki67^+$ cells at the edge of the original wounded area were counted in the absence or presence of Y-27632 eye drops in three different concentrations (1, 3, or 10 mM), and the mean data were then plotted ($n = 6$). Y-27632 eye-drop instillation increased the number of $Ki67^+$ cells at the edge of the original wounded site in a dose-dependent manner. *Scale bar*: 100 μm. $^*P < 0.01$, $^{**}P < 0.05$.